Journal of Cleaner Production 477 (2024) 143853

Contents lists available at ScienceDirect

Journal of Cleaner Production

journal homepage: www.elsevier.com/locate/jclepro

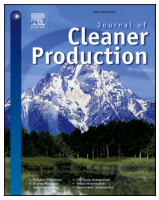

Review

Progress and development of biochar as a catalyst for hydrogen production

Rahul Mishra [a], Chi-Min Shu [a,**], Hwai Chyuan Ong [b,*], Anjani R.K. Gollakota [c], Sunil Kumar [d]

[a] Department of Safety, Health, and Environmental Engineering, National Yunlin University of Science and Technology, Douliou City, Yunlin, 64002, Taiwan, ROC
[b] Department of Engineering, School of Engineering and Technology, Sunway University, Jalan Universiti, Bandar Sunway, 47500, Petaling Jaya, Selangor, Malaysia
[c] Department of Chemical and Materials Engineering, National Yunlin University of Science and Technology, Douliou City, Yunlin, 64002, Taiwan, ROC
[d] College of Sciences and Engineering, University of Tasmania, Launceston Campus, Australia Private Bag 51, Hobart, TAS, 7001, Australia

ARTICLE INFO

Handling Editor: Panos Seferlis

Keywords:
Dark fermentation
Gasification
Photocatalytic water splitting
Pyrolysis
Methane steam reforming

ABSTRACT

The recent progress of the biochar application as a catalyst for the production of hydrogen has been presented in this review. Biochar is a carbon-rich material, which can be produced through different thermochemical conversions (pyrolysis, gasification, and hydrothermal carbonization) using various feedstocks. Biochar has gained attention as a possible catalyst for the production of hydrogen in recent years. It has a distinctive structure and multiple functions and can be accessed widely. The utilization of biochar as a catalyst can significantly improve the hydrogen yield and quality, showing improved catalytic activity and thermal stability. The physiochemical characteristics of biochar are also affected by the different types of feedstocks. Furthermore, the biochar performance can be increased as a catalyst when it is modified with alkali, acid, metal ions, carbonaceous materials, oxidants, purging of gas, and steam. This review presents an overview of the feedstock, production, modification, and characterization methods of the biochar, followed by an elaborate discussion on the application of biochar as a catalyst. This paper addresses the current development of biochar as a catalyst/support for hydrogen production in thermochemical techniques, photocatalytic water splitting, dark fermentation, and methane steam reforming. Overall, biochar catalyst has the potential for a cleaner and more effective energy system.

1. Introduction

Global energy demand is rising immensely owing to the growth of population, urbanization, and industrialization (Mishra et al., 2024). Reserves of fossil fuels have been used to meet this immense need. Around the globe, a substantial amount of energy needs is met by fossil fuels and petrochemicals. Crude oil was reported for ca. 31% of the world's main energy supply in 2020, followed by coal, which was roughly 27% (Kang et al., 2022). The direct or indirect utilization of fossil fuels has an adverse effect on the environment such as smog formation and rise in CO_2 levels (direct effects), global warming, climate change, acid rain, and ozone layer thinning (indirect effects) (Nanda et al., 2016). Global interest is gradually moving toward green energy as a result of these new socioeconomic and environmental issues associated with using fossil fuels. Utilization of alternative and clean energy sources like hydrogen (H_2) will help to reduce the global energy problem and environmental pollution (Lee and Hung, 2012). Therefore, the utilization of H_2 fuel in automobiles will aid in lowering CO_2 emissions compared with fuel derived from petroleum (Hossain et al., 2016). In recent times, the significance of H_2 as a means of clean energy carrier has become apparent (Hossain et al., 2016). In comparison to other fossil fuels, it is more efficient due to its high energy carrier (142 kJ/g) (Pandey et al., 2019).

This clean hydrogen can be generated from numerous techniques such as thermochemical process (pyrolysis or gasification), photocatalytic water splitting, dark fermentation, and methane steam reformation, which are further explained in subsequent sections. Different waste can be transformed into gaseous products particularly H_2 by the thermochemical processes, which are subsequently utilized as a fuel for transportation and others (Mishra et al., 2022). In the present circumstance, the most utilized and favored methods are gasification and pyrolysis (Mishra et al., 2024). Pyrolysis is a thermochemical technique for

Abbreviations: GHG, *Greenhouse Gas*; HTC, *Hydrothermal carbonization*; ZVI, *Zero valent iron*; CNT, *Carbon nanotubes*; BC, *Biochar*; BBNs, *Biochar–based nanotubes*; NPs, *Nanoparticles*; TEOA, Triethanolamine; DRM, *Dry reforming of methane*; SRM, *Steam reforming of methane*; MW, *Microwave*.

* Corresponding author.
** Corresponding author.
E-mail addresses: rahul_s.mishra@yahoo.com (R. Mishra), shucm@yuntech.edu.tw (C.-M. Shu), ong1983@yahoo.com, onghc@sunway.edu.my (H.C. Ong), garkiran@yuntech.edu.tw (A.R.K. Gollakota), sunil_neeri@yahoo.co.in (S. Kumar).

https://doi.org/10.1016/j.jclepro.2024.143853
Received 12 December 2023; Received in revised form 20 February 2024; Accepted 30 September 2024
Available online 2 October 2024

converting waste to syngas, biochar, and bio-oil at a temperature that varies from 300 to 900 °C without oxygen (Mishra et al., 2023b). Gasification converts different waste i.e., carbon sources into various mixtures of gases (H_2, CO_2, CH_4, CO, and hydrocarbons) at a temperature >700 °C using different gasifying agents (air, O_2, steam, and CO_2) (Mishra et al., 2022). The primary products of pyrolysis and gasification are biofuels and syngas (H_2 and CO mixture), respectively. The biofuels are then transformed into syngas using a variety of converting techniques, including pyrolysis followed by in-line reforming, gasification of bio-oil, reforming of bio-oil, etc. Furthermore, a technique for producing H_2 as a solar fuel is sun-driven photocatalysis (Bhavani et al., 2018). In this technique, solar energy is directly captured by the photocatalysts that further transform them into H_2 from water splitting, leading to the reduction of contaminated air/water and CO_2 photoreduction. The most valuable source of energy, solar light, as well as a plentiful supply of water, is used to generate solar fuels. Similarly, polluted water and air have been reduced using an abundance of solar radiation. Moreover, organic wastes such as food waste, agricultural waste, sewage sludge, forestry waste, and wastewater can be used in the dark fermentation process to generate H_2, which can obtain renewable H_2 and waste utilization at the same time (Wang and Yin, 2017). Finally, the methane steam reformation method can also produce H_2 energy. The CH_4 produced during the generation of gas from crude oil is typically released or reinjected. However, such a strategy becomes less prevalent as it has a concern about the greenhouse gas (GHG) effect (Rahimpour and Jokar, 2012). To decrease the impact of CH_4 as a GHG while simultaneously enabling the production of value-added products from syngas, it is preferable to transform CH_4 to syngas comprising H_2 via CH_4 reforming reactions (Tu and Whitehead, 2012; Zeng et al., 2015).

The products produced by these techniques, particularly the thermochemical technique can have more contaminants and lower efficiency of H_2 production. The shortcomings can be solved using catalyst/support, especially carbon catalyst/support. The catalysts have been used to accelerate the necessary reactions for H_2 production. Among them, Ni, Co, Pt, Pd, Co, Fe, and Cu are metal catalysts that have gained prominent interest because of their ability to promote the production of H_2 (Díaz et al., 2021; Karimi et al., 2021). Furthermore, metal oxide catalysts such as cobalt oxide (Co_3O_4), nickel oxide (NiO), cerium oxide (CeO_2), and iron oxide (Fe_2O_3) have shown potential catalytic action in hydrogen-producing techniques (Bielan and Siuzdak, 2023; Mao et al., 2020). Although conventional catalysts are effective for increasing H_2 production, they commonly come with some disadvantages, including limited availability, high costs, and possible environmental effects. Biochar catalysts, on the other hand, are an appealing choice that can be produced sustainably due to their affordability, availability, and environmentally friendly (Nguyen et al., 2024; C. Wang et al., 2020a). Biochar can be utilized as a catalyst/support due to its higher specific area, and the existence of functional groups on its surface. One of the primary byproducts of biomass gasification and pyrolysis is biochar. The previous findings of the biochar's characteristics revealed that it has a greater porosity and surface area, as well as a high concentration of functional groups and minerals like P, Ca, and K (Song et al., 2022). biochar is intriguing as a catalyst and catalyst support, as well as an adsorbent because of these characteristics (Lee et al., 2017). Currently, catalysts supported by biochar have been discovered for syngas production (Mishra et al., 2023a), the generation of biodiesel (Dehkhoda et al., 2010), biogas reforming (Muradov et al., 2012), esterification (Ren et al., 2014), and hydrolysis of biomass (Ormsby et al., 2012). Biochar is an effective catalyst for the production of H_2 in different techniques. For example, Cay et al. (2019) assessed the influence of biochar-type catalysts on the production of hydrogen-rich gas in two-step gasification and reported that the type of biochar had a considerable impact on the H_2 production and gas composition. H_2 and CO_2 proportions in syngas varied based on the feedstock with maximum H_2 production varying from 51.5 to 116.5 mmol/g feedstock. Similarly, Ren et al. (2014) utilized BC catalyst in biomass catalytic pyrolysis for H_2-rich syngas generation and reported high-quality syngas enriched with H_2, CH_4, and CO. Norouzi et al. (2019) produced BC from different waste, then it was loaded with iron oxide and assessed the photocatalytic production of H_2 under visible light. After biochar was loaded with metal, the surface area improved, leading to better photocatalytic activity. Zhao et al. (2021b) investigated the biochar role in the increased generation of bio-hydrogen through saccharification and fermentation of cornstalk at a time. Zhao et al. (2023) utilized BC in a study for catalytic methane reforming. Using activated BC, approximately 46% of CH_4 conversion with about 396 mmol/gcat of H_2 output was reported.

Several review papers are present that focus on the production of bio-oil using biochar catalysts, however, there is a lack of review papers on the utilization of biochar as a catalyst in gas production, particularly hydrogen. Thus, the objective of this review paper is to offer in-depth insights into the utilization of biochar as a catalyst for hydrogen production in different techniques such as thermochemical techniques, photocatalytic water splitting, dark fermentation, and methane steam reforming. This review also reveals the influence of several biochar conversion and modification techniques on the physicochemical characteristics of the produced pristine biochar and modified biochar. It provides a summary of recent advancements and prospective applications of biochar. This review paper could provide useful information for industries and researchers who seek to conduct research on biochar application as well as hydrogen production. The dependence on fossil fuels for energy production can be substantially decreased with further improvement and integration of biochar, as well as solving environmental issues like GHG emissions and climate change.

2. Biochar feedstocks and production techniques

There is a growing interest in using forest waste as a feedstock for biochar generation because of its availability and low price. Additionally, converting biomass waste into biochar will lower the expenses associated with the management of waste. The estimated annual global amount of agricultural residues is 500 MT (Kumar et al., 2022). These are typically wastes gathered from bioenergy production and agricultural harvesting. (Kumar et al., 2022). Animal waste is another possible feedstock resource. Biochar generated from dairy compost and poultry litter contains huge quantities of debris and inorganic fragments suitable for limiting metal ions (Kumar et al., 2022; Romero et al., 2021). Besides, many different sources that have been applied to produce biochar including macroalgae (Michalak et al., 2019), date stone (Chakraborty et al., 2020), seaweed (Cao et al., 2021), olive pit (Campos and De la Rosa, 2020), oyster shell (Lian et al., 2021), tobacco stalk (Yu et al., 2021), cinnamon and cannabis (Omidi et al., 2019), orange peel (Adeniyi et al., 2020), pig bone (Deng et al., 2021), plastics (Mishra et al., 2023a), brewer's spent grain (BSG) (Yoo et al., 2021), residues of herbal medicine (H. Wang et al., 2021), cow dung (Yao et al., 2021), and cornstalk (Zhao et al., 2021b). There are various ways to generate biochar from these feedstocks, including pyrolysis, gasification, hydrothermal carbonization, etc., Fig. 1 shows the differences among the different processes i.e., gasification, fast pyrolysis, and slow pyrolysis for biochar production (Brewer et al., 2009; Mohan et al., 2014). Biochar production from various feedstocks at different temperatures with different techniques as well as its proximate and ultimate analysis is presented in Table 1.

2.1. Pyrolysis

Biomass is thermally broken down during pyrolysis without the presence of oxygen (Mishra and Kumar, 2023). The majority of feedstock decomposition in this process occurs in two phases i.e., primary and secondary phases. Dehydration, dehydrogenation, and decarboxylation occur during the first step (Patel et al., 2020). After the primary reaction is finished, the secondary reaction begins, breaking down larger molecules and turning materials into gases and biochar. Depending on

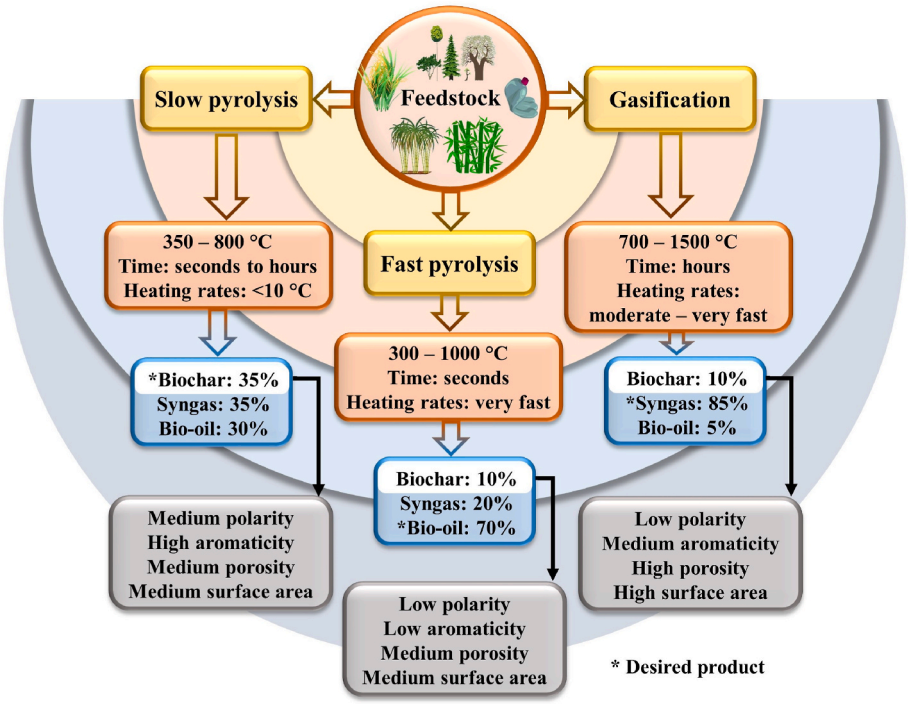

Fig. 1. Differences among different processes for biochar production.

the circumstances of operation, there are primarily two types of pyrolysis i.e., slow pyrolysis and fast pyrolysis. Slow pyrolysis is the process of heating at a temperature of 300–800 °C for an extended period i.e., seconds to hours at a heating rate <10 °C min^{-1} (Fig. 1) (Mohan et al., 2014). The prolonged pyrolysis procedure improved the generation of biochar by providing an environment that is suitable for secondary mechanisms. Fast pyrolysis involves heating biomass promptly for a short duration of time i.e., 0.5–2 s at a higher temperature of 300–1000 °C and a greater heating rate of 10–1000 °C/s (Fig. 1) (Alvarez et al., 2015). The three primary end products of pyrolysis are syngas, biochar, and bio-oil (Te et al., 2021). The chemical pathway of biochar production from biomass through pyrolysis is shown in Fig. 2. Biochar can be used as a catalyst, fuel, and adsorbent. The syngas contains H_2, CO_2, CO, CH_4, etc. which can be utilized by gas turbines after processing. The bio-oil, which can be utilized in fuel boilers, is composed of nitrogenous compounds (amine, pyridine, pyrazine, etc.), aromatic and aliphatic hydrocarbons, phenolic compounds, alcohol, and water (Patel et al., 2020). Porosity, surface area, and functional groups are affected by the temperature of pyrolysis. As temperature rises, ester and aliphatic alkyl groups in organic compounds break down, increasing porosity and surface area as well as eliminating pore-blocking materials (Al-Rumaihi et al., 2022; Chi et al., 2021). Low-temperature biochar has a structure similar to graphene but with fewer functional groups and is hydrophilic. High temperatures make biochar hydrophobic, rearrange its functional groups, and provide new ones, such as pyridine, phenol, lactone, carboxyl, etc. These new groups can serve as electron acceptors and donors (Chi et al., 2021). The output and quality of biochar are also influenced by the feedstock types. For example, about 30% of biochar was produced using forestry plant pyrolysis while lignin-based feedstocks produced about 45.69% of biochar, showing that lignin content affected biochar output (Toloue Farrokh et al., 2018).

2.2. Gasification

The gasification technique involves converting biomass into gaseous products i.e., H_2, CH_4, CO, etc. at 500–1400 °C when there is insufficient oxygen. By passing different gasifying agents i.e., CO_2, steam, air, O_2, and a specific mixture of gases, the gaseous products' production can be increased (Mishra et al., 2022). More than 50% of biomass is converted into gases using this technique, and the generated small amount of biochar is impervious to chemical oxidation (Yaashikaa et al., 2020). A possible pathway of biochar production from biomass through the gasification process including graphical pathway and reactions is shown in Fig. 3. Compared to biochar generated by pyrolysis, gasification-produced biochar typically has a lesser functional group i.e., carboxyl, carbonyl, and hydroxyl groups, as well as a smaller surface area (Peterson and Jackson, 2014). The equivalence ratio (ER) also affects BC's output and quality. A greater ER means more oxygen is introduced into the gasifier, which may affect the characteristics of the biochar. A rise in ER to 0.6 from 0.1 caused a lessening in the carbon content and biochar output from about 88.17% to 71.6% and 0.22 to 0.14 kg/g, respectively (Yao et al., 2018). Because of the high concentration of oxygen, biochar's output and mechanical strength are decreased and ash content is elevated. The biomass type used in the gasification method largely determines the quantity of alkali and alkaline earth metals in the produced biochar (Ahmed et al., 2021).

2.3. Hydrothermal carbonization

Hydrothermal carbonization (HTC) is utilized for low-moisture biomass material and differs significantly from pyrolysis and gasification (J. Lee et al., 2018). As biomass HTC is typically carried out under water pressure at a temperature between 180 and 250 °C, it is considered a low-cost technique for BC production (Kumar et al., 2022). A possible pathway of biochar production from biomass through the hydrothermal carbonization process is shown in Fig. 4. The ratio of water to biomass, pressure, residence duration, and temperature are the primary factors that determine the product quality of produced biochar. The ideal HTC-process product, hydrochar, has an output of between ca. 40 and 70 wt% (Yan et al., 2010). There are more oxygen-containing groups on the surface of hydrochar, indicating a greater degree of aromatization (Sevilla and Fuertes, 2011). Further, the hydrochar's dewatering and drying process was described by Oliveira et al. (2013). Reusing the water used in the technique is possible and can lessen its

Table 1
Biochar production from various feedstocks at different temperatures with different techniques as well as its proximate and ultimate analysis.

Feedstock	Technique	Temperature (°C)	Proximate analysis (%)				Ultimate analysis (%)				Surface Area (m^2 g^{-1})	Reference
			AC	VM	FC	MC	C	H	N	O		
Groundnut shell	Pyrolysis	500	24.71	13.92	59.24	2.13	89.03	2.19	0.21	4.48	–	Rathod et al. (2023)
Mallee wood	Pyrolysis	500	3.66	28.20	68.14	2.41	76.08	2.34	0.39	21.19	–	Shen and Wu (2023)
Sugarcane	Pyrolysis	550	14.9	0	83.3	1.85	52.7	6.76	0.47	–	–	Singh et al. (2021)
		450	20.1	0	78.5	1.39	57.2	1.88	0.86	–	–	
Bamboo	Pyrolysis	550	6.85	7.37	85.3	0.36	66.1	3.62	1.0	–	–	
		450	8.09	5.30	85.4	1.15	63.1	1.47	0.75	–	–	
Neem	Pyrolysis	550	9.68	15.1	73.5	1.76	78.1	1.99	0.7	–	43.9	
		450	6.96	18.4	72.5	2.15	72.8	2.50	0.75	–	–	
Pine needles	Pyrolysis	700	18.74 ± 0.57	–	–	0.01 ± 0.00	93.67	0.62	3.64	2.07	390.52	Ahmad et al. (2013)
		500	11.77 ± 0.18	–	–	0.01 ± 0.00	90.10	2.06	4.10	3.74	13.06	
		300	7.20 ± 0.31		–	0.01 ± 0.00	84.19	4.37	3.88	7.57	4.09	
Miscanthus	Gasification	1000	12.99	8.04	78.97	–	91.74	2.20	0.31	5.41	981.75	Tian et al. (2021)
Marc of grape	Gasification	1200	27.28	26.46	46.26	5.89	57.46	2.32	2.30	37.55	3.64	(Hernández et al., 2020)
Sargassum horneri	Gasification	800	25.73	–	74.27	–	88.96	6.13	2.75	1.79	–	(J. Li et al., 2019)
Common reed	Gasification	800	8.48	7.48	84.04	–	94.97	1.72	1.81	1.5	–	
Corn stalks	Gasification	800	30.34	8.91	60.75	–	90.69	0.26	1.14	7.47	–	
Hardwood chips	Gasification	790	1.119	79.85	19.031	25	49.817	5.556	0.078	43.425	–	Tauqir et al. (2019)
Sewage sludge	Hydrothermal carbonization	100	30.14	58.86	10.60	0.40	34.79	4.74	4.44	24.26	–	Silva et al. (2020)
Chlorella vulgaris	Hydrothermal carbonization	180–250	24.7	29.0	43.8	2.5	27.4	7.0	5.5	59.7	–	Khoo et al. (2020)
Canna indica	Hydrothermal carbonization	240	14.13 ± 0.32	–	–	–	57.23	5.52	3.10	20.04	–	Cui et al. (2020)
	Hydrothermal carbonization	220	12.78 ± 0.18	–	–	–	52.69	5.64	2.53	26.37	–	
	Hydrothermal carbonization	200	11.83 ± 0.11	–	–	–	47.50	5.53	2.13	33.02	–	
Hydrocotyle verticillata	Hydrothermal carbonization	260	16.68 ± 0.67	–	–	–	62.28	5.99	4.72	10.34	–	Cui et al. (2020)
	Hydrothermal carbonization	240	14.98 ± 0.46	–	–	–	59.21	5.93	4.51	15.38	–	
	Hydrothermal carbonization	220	14.52 ± 0.39	–	–	–	53.24	5.85	3.88	22.51	–	

environmental impact and increase energy output (Oliveira et al., 2013). The effects of the HTC reaction period, temperature, and the proportion of biomass to water on tomato peels were investigated by Sabio et al. (2016). The findings exhibited that reaction period, and temperature, rather than the biomass/water ratio, impacted biochar output and vitality densification. The pyrolysis of biochar is different from the method used for producing hydrochar. The long-chain cellulose is broken down into atomic weight-smaller compounds (oligomers), afterward to glucose that further isomerizes and produces fructose (Kumar et al., 2022). After this, the products of hydrolysis undergo a series of isomerization reactions followed by drying out, creating a significant amount of 5-HMF and associated products. With condensation of intermolecular dehydration and reverse aldol, extra polymerization has also been observed (Funke and Ziegler, 2010). With polyfuranic rings, hydrophobic cores, and hydrophilic shells, a polyaromatic structure connects the hydrochar produced from cellulose.

3. Biochar modification

Lower surface area, i.e., less than 150 m^2/g, and porosity, as well as limited surface functionality with −OH, C=O, and C−O, were found in the biochar generated from biomass pyrolysis, which may restrict its broad range of uses as a beneficial catalyst (Liu et al., 2011; Mullen et al., 2010). However, modification of biochar's functionality and porosity of surface can be carried out to serve as a platform for the production of different functionalized carbon substances (Liu et al., 2015). The biochar's large surface area and porosity enable it to load with active phases, which can greatly increase the catalytic activity of the material during processes. Additionally, the biochar's functionality can offer more active catalytic sites. The general strategies for biochar modification and its impact on different properties of biochar are shown in Fig. 5.

3.1. The modification of biochar before use as the catalyst/support

3.1.1. Physical modification

The structure, pore volume, and surface area of biochar can be improved via physical modification (H. W. Lee et al., 2018). Biochar is physical or gas-activated using gas, such as CO_2 and steam at a comparatively higher temperature of >700 °C (Cha et al., 2016). When oxygen in the water during steam activation interacts with the carbon on the surface of biochar produces surface oxygen and hydrogen (Yaashikaa et al., 2019). When the hydrogen comes into interaction with the carbon surface, it then generates the surface hydrogen complex. The surface hydrogen complex then goes through oxidation during the activation, resulting in the production of CO_2 and hydrogen. Various functional groups (i.e., ether, hydroxyl, phenolic, carboxylic, etc.) accumulate on the surface of biochar. In addition, this mechanism encourages self-polymerization. The carbon concentration of the activated

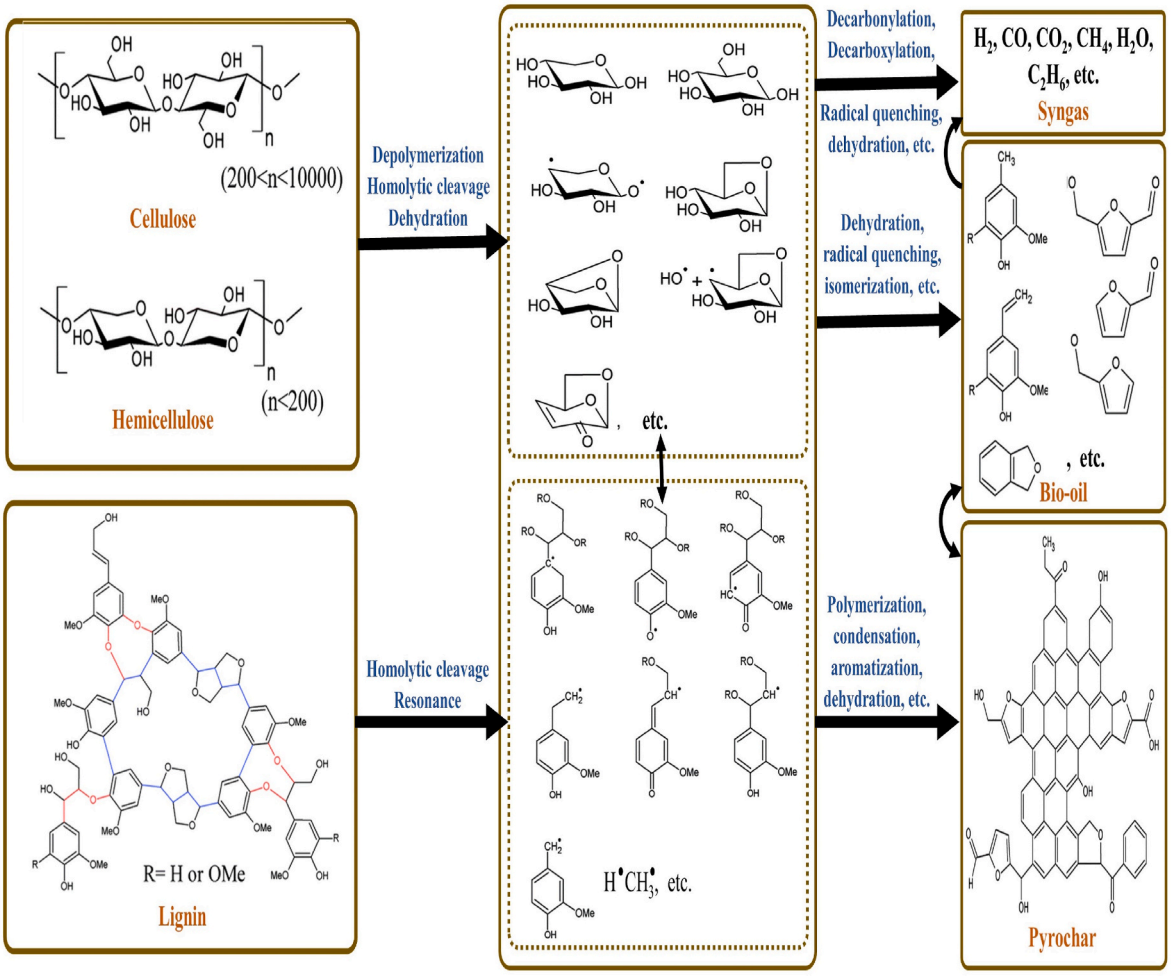

Fig. 2. Chemical pathway of biochar production from biomass through pyrolysis. Reproduced from (X. Cao et al., 2017) with permission from the Royal Society of Chemistry.

biochar is high, it has a large surface area, as well as porosity. According to Lam et al. (2020), the process of physical activation depends on time and temperature. Longer time and greater temperatures result in improved porosity growth. Biochar was generated from willow by Kołtowski et al. (2017), which was further activated by steam at a temperature of 800 °C for 78 min in an N_2 atmosphere. This research revealed that steam activation greatly increased the biochar's porosity and surface area. With a 30-min activation period, the steam activation of different agricultural residues was performed by González et al. (2009) in a nitrogen atmosphere at 850 °C. Compared with the inactivated biochar's surface area, i.e., about 42–280 $m^2\ g^{-1}$, steam-activated biochar had a greater surface area i.e., about 601–1080 $m^2\ g^{-1}$. Furthermore, following the application of steam activation, the micropore volume also improved. In steam, biochar was modified at 700 °C for a time of 1h by Cha et al. (2010) and it was reported that total pore volume enhanced to ca. 0.164 from 0.092 $cm^3\ g^{-1}$. Overall physical activation significantly increases biochar's pore volume and surface area.

3.1.2. Chemical modification

The most popular method for activating biochar is chemical activation. Despite requiring more time and energy than physical activation (H. W. Lee et al., 2018), it is preferable because it has greater activation efficiency (Cha et al., 2016). Though the use of chemical activation has many disadvantages, including equipment corrosion, chemical recycling, and secondary pollution due to its acidic characteristics (X. Cao et al., 2017). Nevertheless, the chemicals can inhibit the production of tar and remove volatile substances, as well as partial carbon molecules from biochar (Lam et al., 2020). Numerous research has found that chemical activation increases biochar's surface area and pore volume, which are further discussed in the subsequent sections.

3.1.2.1. Alkaline activation. Alkali chemicals like KOH and NaOH can activate raw biochar. Under inert gas flow, the biochar is heated at the temperature of 500–1000 °C after impregnation with KOH or NaOH. It has been shown that the porosity of activated biochar can be adjusted by the impregnation time and the quantity of alkaline (Liu et al., 2015). Greater alkaline concentrations can result in greater porosity along with increases in pore volume and surface area (Li et al., 2014). Biochar at high temperatures releases some volatiles, such as H_2O and CO_2, which can be absorbed by KOH to produce K_2CO_3 (Reaction (1)). As a result of its reaction with carbon (C), KOH can produce H_2 and CO (Reaction (2)). The gaseous species' escape can create a variety of porous shapes. The freshly generated K_2CO_3 can combine with the C to generate more gases as the temperature rises, such as K and CO, which results in the development of larger pores (Reactions (3) and (4)) (Wang and Kaskel, 2012).

$$2KOH + CO_2 \rightarrow K_2CO_3 + H_2O\uparrow \quad (1)$$

$$2C + 2KOH \rightarrow 2CO\uparrow + 2K\uparrow + H_2\uparrow \quad (2)$$

$$K_2CO_3 + C \rightarrow K_2O + 2CO\uparrow \quad (3)$$

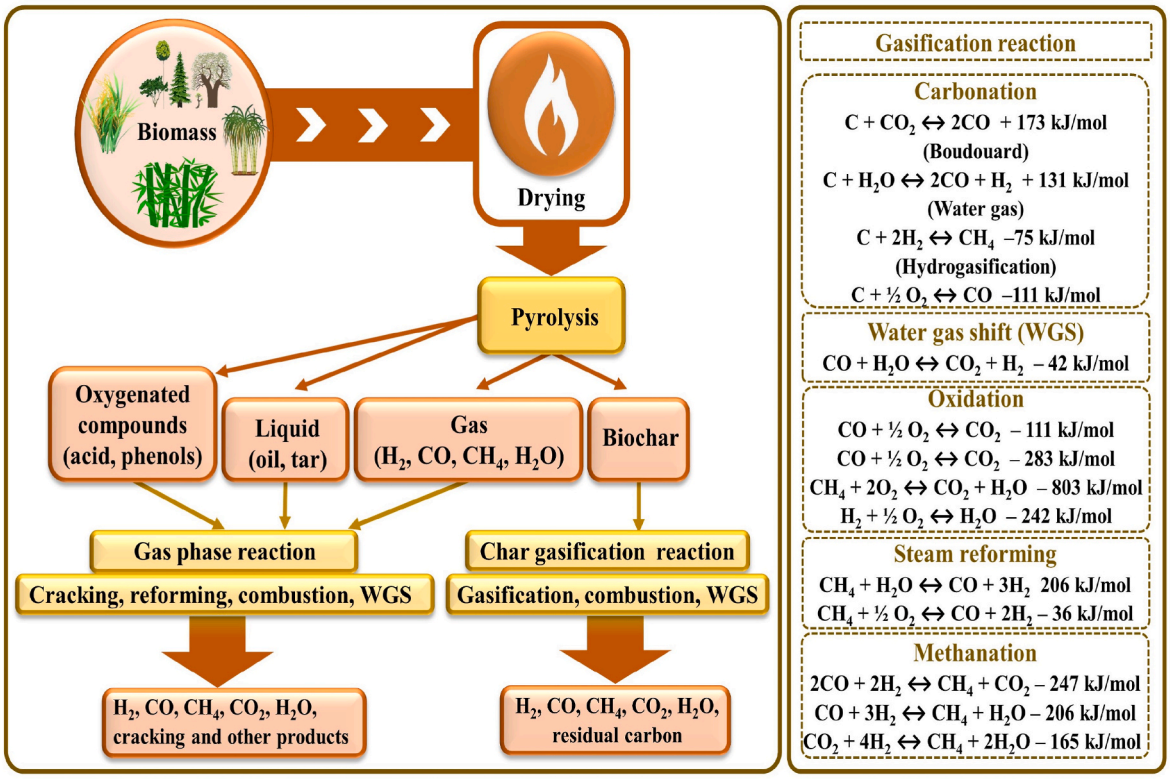

Fig. 3. Possible pathway of biochar production from biomass through gasification process including graphical pathway and reactions.

$$K_2O + C \rightarrow 2K\uparrow + CO\uparrow \quad (4)$$

A 1:1 ratio of KOH was used by Cha et al. (2010) to study the activation of biochar. The results confirmed that the biochar's pore volume enhanced to about 0.422 $cm^3\ g^{-1}$ from 0.092 $cm^3\ g^{-1}$ and its surface area increased to about 772.3 $m^2\ g^{-1}$ from 139.5 $m^2\ g^{-1}$. In the research done by Bhandari et al. (2014), switchgrass was gasified to produce biochar in the fluidized bed and downdraft gasifiers. Each biochar was further activated by combining it with KOH before the sonication process. The total pore volume and surface area were greater in the downdraft gasifier than fluidized bed gasifier. The research showed that in comparison to biochar generated in different gasifiers without modification, basic activation was a successful method for raising the overall quality of biochar as it increased the total pore volume and surface area.

3.2. *Surface functionality of biochar for catalysis*

3.2.1. *Acid modification*

The primary functional group in solid acidic compounds is sulfonic (-SO_3H). The most popular technique to generate acids-based biochar is biochar's surface sulfonation using concentrated H_2SO_4 or its substitutes such as chlorosulfonic acid and oleum (Nakajima and Hara, 2012). A common class of solid Brønsted acids was represented by biochar, which contained the -SO_3H group, as well as about 2.5 mmol H^+/g of acid sites' densities could be achieved (Shan et al., 2020). The high acid site (-COOH, -SO_3H, and -OH groups) on the surface can be responsible for the high stability and catalytic performance of produced acid catalysts, which demonstrated superior catalytic activity for a variety of acid-catalyzed processes, including the hydrolysis and esterification reactions (Bhatia et al., 2020; Yu et al., 2011).

3.2.2. *Loading of functional materials*

Zero-valent iron (ZVI), carbon nanotubes (CNT), graphitic carbon nitride (g-C_3N_4), graphene oxide, graphene, and other functional materials can be effectively loaded onto BC surface to integrate their benefits (Kumar et al., 2020). For instance, g-C_3N_4 has been extensively utilized in environmental photocatalysis as a metal-free polymeric semiconductor with an excellent response to visible light (Zhang et al., 2018). Owing to its efficient photogenerated carrier separation and excellent absorption characteristics of biochar, the g-C_3N_4-supported biochar catalyst could demonstrate greater photocatalytic performance than pure g-C_3N_4 (Lyu et al., 2020).

3.2.3. *Loading of metal nanoparticles*

After biomass pyrolysis, it is possible to produce the majority of biochar-based composites with metal oxide bonded onto BC structure. Typically, metal salt solutions are used to saturate biochar, which causes metal ions to stick to its pores and surface. Their corresponding metal oxides accumulate on the biochar surface after additional thermochemical processing. For instance, biochar is frequently utilized for thermochemical processes when loaded with Ni, Fe oxides, or bimetallic nanoparticles based on Fe-Ni (Nguyen et al., 2016; Wang et al., 2011). The most common metal photocatalysts are Zr, Sn, Zn, and Ti oxides (Lyu et al., 2020). Besides, metal salts such as Cu $(NO_3)_2$ and $AgNO_3$ can be used for the pretreatment of biomass before pyrolysis (Liu et al., 2016; Tian et al., 2016). Metal ions can penetrate the interior of biomass after it has been dissolved in a solution of metal salts, in addition to attaching to its surface. The metal particles may change into metal or nano-metal oxide during the following pyrolysis process. As a result, metal-ion-impregnated biomass may develop nanocomposites based on biochar (Liu et al., 2020). It is noteworthy that when using biochar to remove pollutants from water, a magnetic medium (Fe_3O_4 or Fe_2O_3) can mix with it to create magnetic material through chemical co-precipitation or pyrolysis activation (X. Li et al., 2020; S. Wang et al., 2019). Because of its acquired magnetic property, biochar is reusable after each reaction.

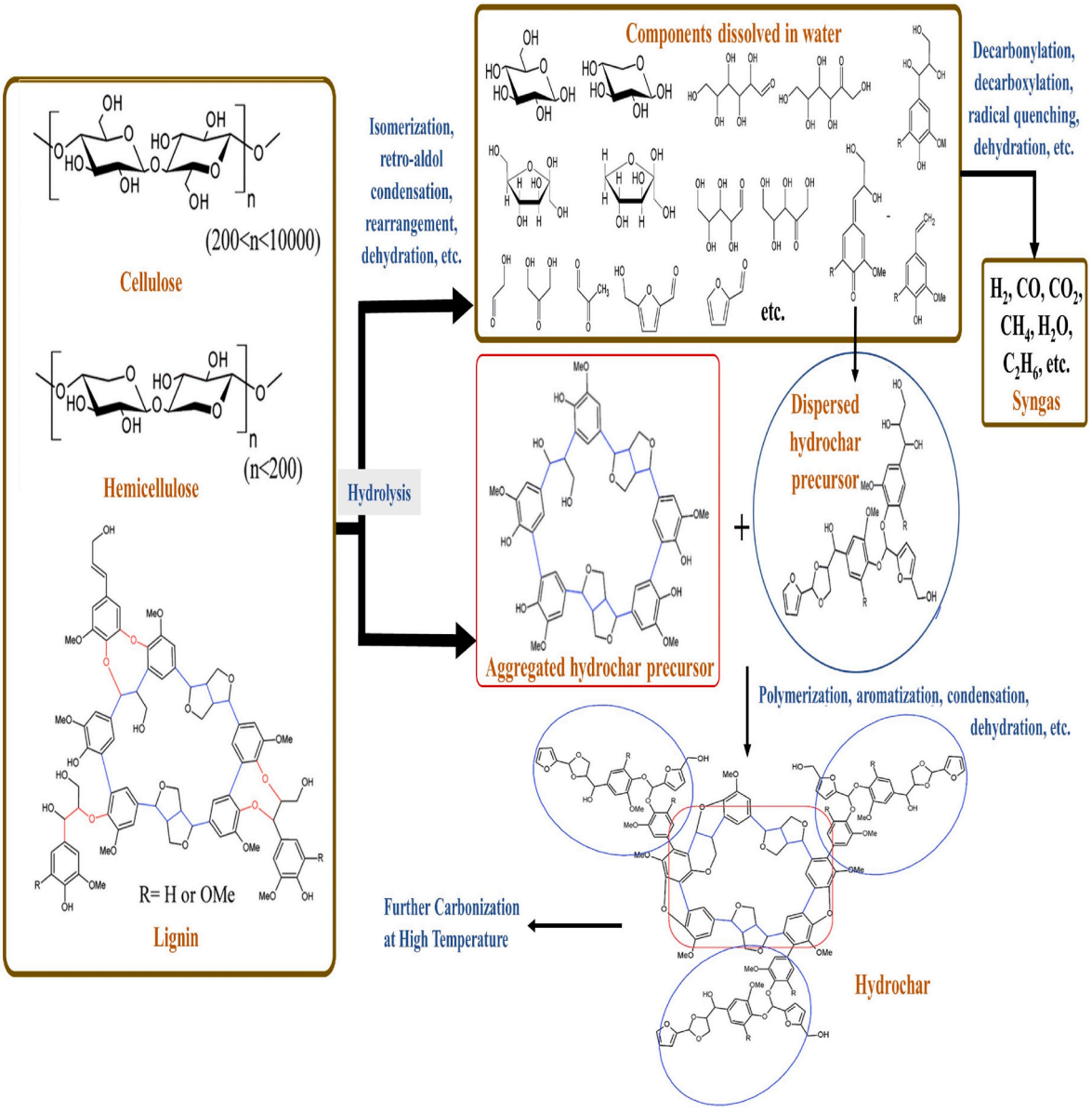

Fig. 4. Possible pathway of biochar production from biomass through hydrothermal carbonization process. Reproduced from (X. Cao et al., 2017) with permission from the Royal Society of Chemistry.

3.2.4. Other surface doping

It has been demonstrated that carbonaceous compounds like biochar's electronic structure can be altered by heteroatoms (P, B, S, and N). It is believed to be a practical method for enhancing the metal-free carbon catalysts' ability for catalysis. In particular, electron transfer is facilitated by the N atom in the catalytic system throughout the process and enhances electronic interaction between support and metal-active substances (Y. Cao et al., 2017). Advanced oxidation methods frequently use biochar catalysts that have been doped with N. The N-doping proved to enhance biochar's positive-charged C atoms, which increases the bonds between the catalyst and peroxymonosulfate in the catalytic breakdown of metolachlor (Ding et al., 2020).

4. Characterization of biochar-derived catalyst

Characterizing the biochar is essential after preparation to comprehend its chemical characterization and morphology. In terms of a summary, typical methods of analysis for biochar include thermogravimetric analysis (TGA), Raman spectroscopy, scanning electron microscopy (SEM), temperature-programmed desorption (TPD), solid-state nuclear magnetic resonance (NMR), extended X-ray absorption fine structure (EXAFS), X-ray photoelectron spectroscopy (XPS), Fourier transform infrared spectrometry (FTIR), Brunauer–Emmett–Teller (BET), and Xray diffraction (XRD) was briefly discussed. Besides, other analysis techniques for biochar characterization of biochar are shown in Fig. 6 in the form of a flow chart.

The physical morphological alterations that took place in the biochar after the activation stages were examined using SEM analysis. A beam of electrons is used to scan the sample surface in this technique. The substantial morphological differences between biochar and activated biochar, such as the increment of surface area and the development of porosity, are demonstrated by SEM analysis. To assess the original and functionalized biochar's thermal stability, TGA is utilized. With the help of this technique, it is possible to understand more about the chemical and physical processes that are present in the materials being characterized, such as thermal decomposition and chemisorption. It was noted after reviewing the literature, the TGA should be carried out on biochar and its findings can be evaluated to comprehend the efficacy of the

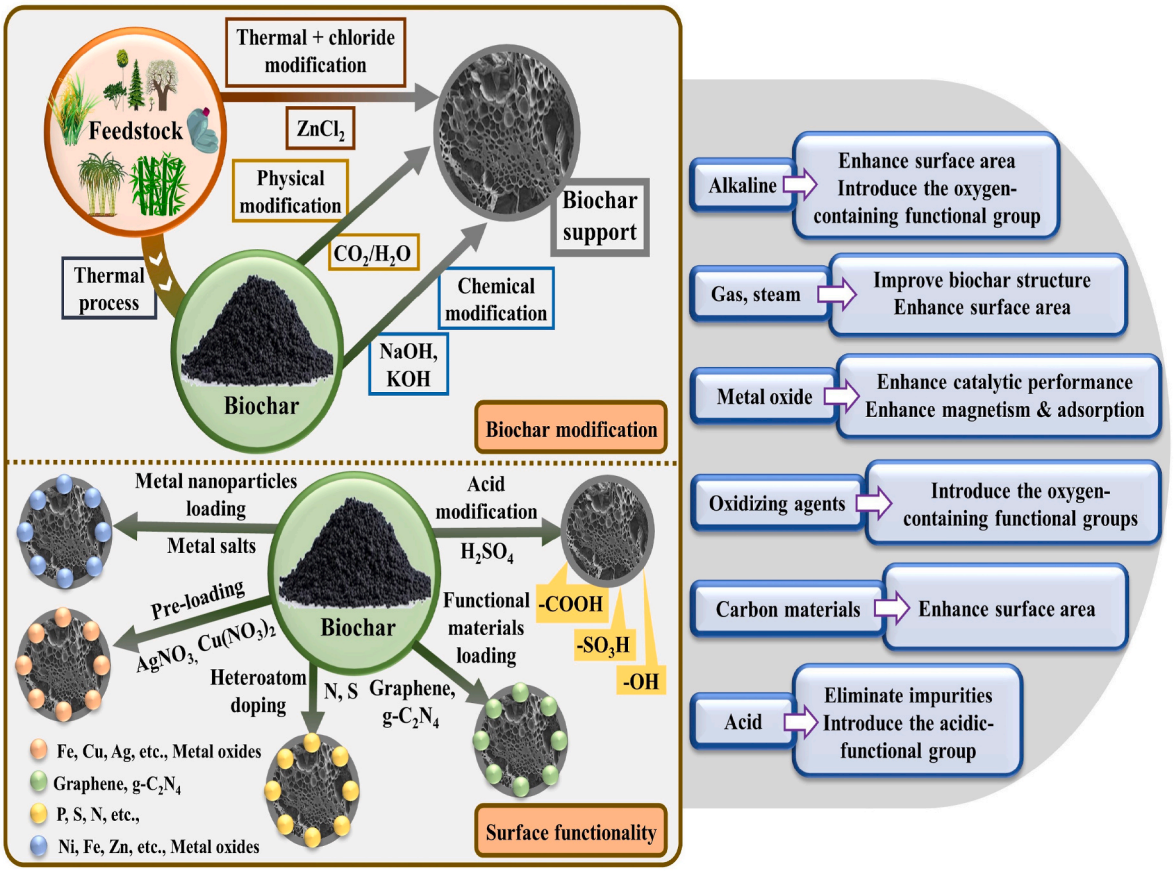

Fig. 5. General strategies for biochar modification and its impact on different properties of biochar.

applied activation method and thermal stability. Raman spectroscopy is a method that gives insight into the chemical composition and molecule interactions of C-species elements (Liu et al., 2020). In a study, a G peak and a D peak were visible in the biochar produced from corn stalks at 1590 cm^{-1}, and 1380 cm^{-1}, respectively (Huang et al., 2019). Furthermore, R was used to indicate the ratio of D peak intensity (ID) to G peak intensity (IG) with a greater R-value indicating a higher level of disorder. The distribution and density of alkaline or acid in the heterogeneous catalyst are determined using TPD (Balajii and Niju, 2019). By Zeeman splitting of the nucleus spin level in the existence of an external magnetic field, NMR can detect the amount of protonated or non-protonated carbon and the carbon aromaticity in biochar (Wan et al., 2020). EXAFS can describe the poly-aromatic composition of biochar using the multiple scattering resonance process (Kumi et al., 2020). To evaluate the efficiency of the specified preparation or activation technique accountable for the catalytic activity, the surface characteristics of the modified and original biochar, such as pore size distribution, the specific surface area, and pore structure must be identified. BET examination includes the gas molecules' physical adsorption usually N_2 on the biochar surface (Wen et al., 2023). A variety of materials can be characterized using the quantitative surface analysis method known as XPS, which can be used to determine the chemical composition, elemental composition, and element's electronic state that make up a substance. The elemental makeup at the catalyst surface is measured with an X-ray beam under an ultra-high vacuum. An analytical method used to identify polymeric, inorganic, and organic compounds is called FTIR (Xie et al., 2023). Infrared light is used in this technique to scan the materials and examine their chemical composition. The modified or functionalized, and original biochar show the functional group changes. Additionally, it displays each group's stretching and vibrational modes that were found in the biochar. The different functional groups that contribute to the generated catalyst's high catalytic activity can be identified using the FTIR technique. An effective nondestructive method used to examine solid materials is XRD (Pak et al., 2023). A monochromatic X-ray beam is used in this technique. It offers an extensive amount of data on test samples, primarily on crystallinity, typical particle size, and phases. It also reveals the solid and amorphous characteristics of samples of original and functionalized biochar. The XRD tests show the biochar nature i.e., crystalline and amorphous as well as the presence of chemical groups on the modified biochar.

5. Hydrogen production using biochar catalyst

5.1. *Biochar as a catalyst in the thermochemical process*

One of the most efficient ways to produce H_2 from waste such as biomass, and plastics is the thermochemical process, particularly pyrolysis, and gasification (Mishra et al., 2023b). With limited use in the transformation of biomass and plastic waste, thermal pyrolysis and gasification are temperature-dependent techniques. Catalysts are used in catalytic pyrolysis and gasification processes for the breakdown of plastics. These processes use lower reaction temperatures and less energy to maximize product quality and conversion rates (Mishra et al., 2022). Catalysts play an important role in the catalytic procedure for plastics and biomass conversion for H_2 production. The most popular metal catalyst is nickel (Ni), which is renowned for its superior tar-reduction efficiency and increased H_2 production. However, Ni-based catalysts are to some extent costly, which is one of the major factors driving up the process' overall cost. In addition, deactivation happens as a result of coking (Asadullah et al., 2002) and the Ni particle development, both of which have a detrimental effect on the catalyst

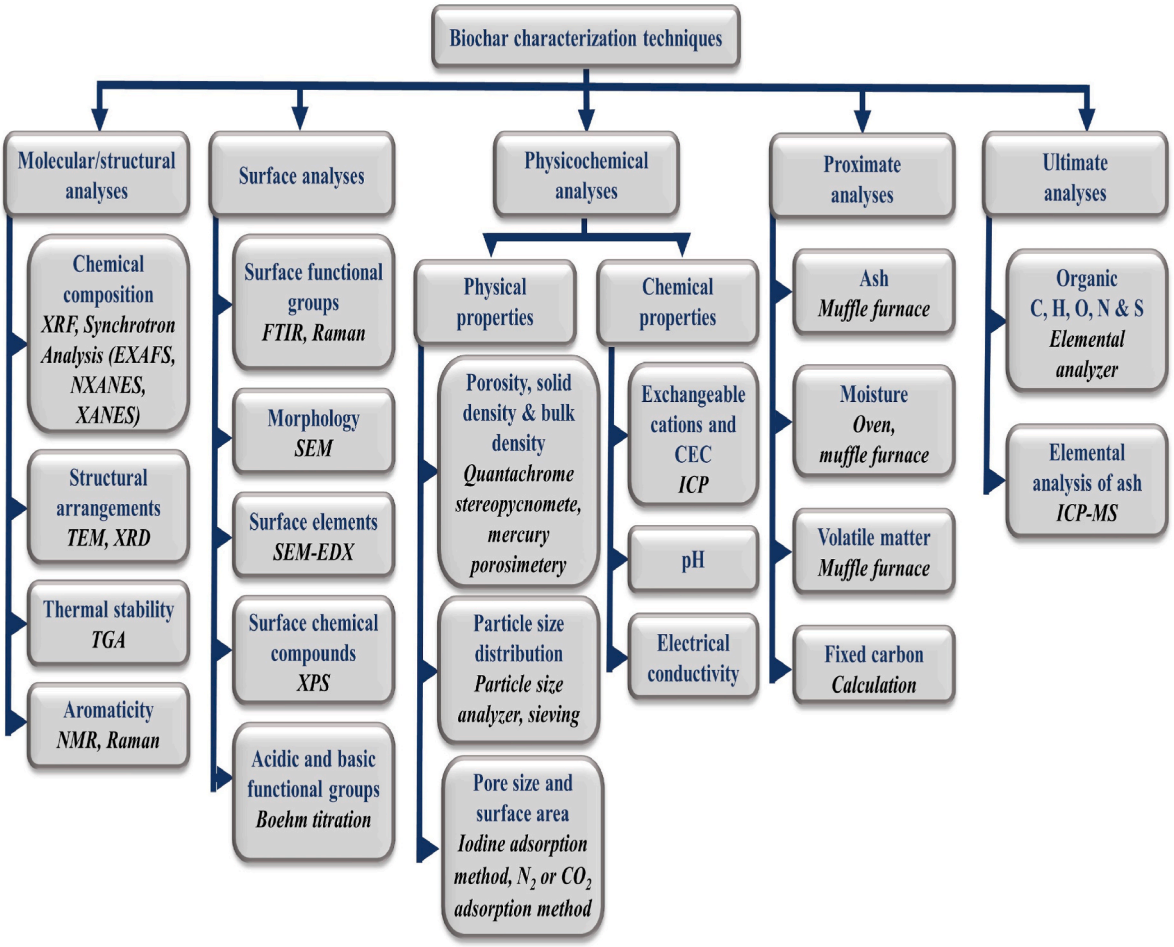

Fig. 6. Different analytical approaches for characterization of biochar including physical and chemical properties (Igalavithana et al., 2017). XRF: Xray fluorescence, TGA: thermal gravimetric analysis, XRD: X-ray diffraction, TEM: transmission electron microscopy, ICP-MS: inductively-coupled plasma mass spectroscopy, NMR: nuclear magnetic resonance spectroscopy, FTIR: Fourier transform infrared spectroscopy, SEM: scanning electron microscopy, XPS: X-ray photoelectron spectroscopy, SEM-EDX: SEM with energy-Dispersive X-ray spectroscopy, XANES: X-ray absorption near-edge structure spectroscopy, NEXAFS: near-edge X-ray absorption fine structure spectroscopy, EXAFS: extended X-ray absorption fine structure spectroscopy.

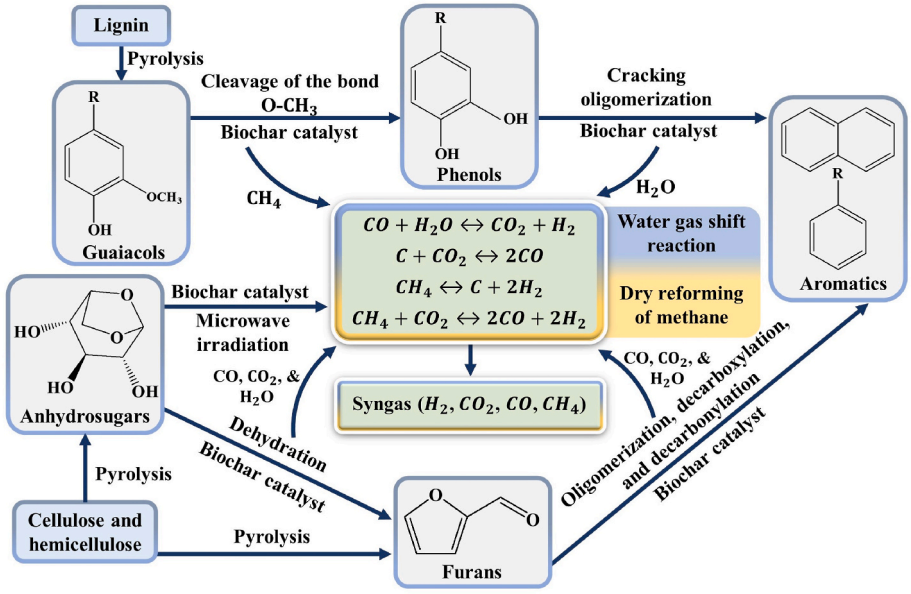

Fig. 7. The reaction pathway of biomass catalytic thermochemical process using biochar as a catalyst. Reproduced from (Ren et al., 2014) with permission from the Royal Society of Chemistry.

activity. This issue can potentially be resolved by adding promoters like Li, Na, and Ca to Ni-based catalysts (Weerachanchai et al., 2009). The presence of metals like K and Ca (Hu et al., 2015) in biomass and their concentration in biochar, which facilitates the water gas shift reaction (Shen, 2015) is widely recognized. Thus, the application of biochar as a support for metal catalysts can be seen as an effective way to minimize the coking-induced deactivation of a Ni-based catalyst (Xiao et al., 2013). A low-cost carbonaceous substance known as biochar can be utilized as a catalyst/support (Sun et al., 2018). Metal-supported catalysts such as Ni/activated carbon, Ni/biochar (Yao et al., 2016), Ni/dolomite (Waheed and Williams, 2013), and alkali-catalyzed (Imai et al., 2018) can be utilized for improving H_2 production. The reaction pathway of the biomass catalytic thermochemical process using biochar as a catalyst is shown in Fig. 7 (Ren et al., 2014). Some research on hydrogen production from different feedstock in the thermochemical technique using biochar as a catalyst is shown in Table 2. Highly stable biochar catalysts were used by C. Wang et al. (2020b) to efficiently pyrolyze plastic wastes. Roughly 78 vol% of H_2 concentrations were noted in the gas output. The biochar could increase H_2 production while simultaneously reducing CH_4 generation. Furthermore, a comprehension of the reaction mechanism was also addressed. The dominant mechanisms for the catalytic and thermal cracking of hydrocarbons, respectively, have been demonstrated to be the carbonium ion and free radical reaction mechanisms. Firstly, the long-chain alkanes (i.e., LDPE) thermal decomposition occurs and the process is dominated by the mechanism of the free radical reaction. The three sequential phases i.e., chain initiation, propagation, and termination occur in the free radical reaction. The effect of heat results in the generation of numerous smaller free radicals with CmHn•, CH_3•, and H• in the first phase. The propagation phase of the newly formed radicals then contains the reactions of isomerization, β-scission, and H-abstraction. The H-abstraction is also known as the H-transfer, which can cause interactions between existing radicals and hydrocarbons to produce H_2, CH_4, etc., and new radicals (C. Wang et al., 2020b). Ren et al. (2014) generated hydrogen-rich syngas via biomass catalytic pyrolysis by biochar catalyst. For catalytic pyrolysis of biomass using biochar as a catalyst, high-quality syngas that is abundant in H_2, CH_4, and CO were produced. In their research, two main reaction mechanisms have been reported to produce H_2 and CO. Without biochar, the syngas from the decomposition of Douglas fir was primarily made up of short-chain hydrocarbons, CO, CH_4, and CO_2. Based on dry biomass, the water content of raw bio-oils varied from about 17.2 to 24.7 wt%. The biochar catalyst was filled with CO and water. Improved levels of hydrogen (from zero H_2 without a biochar catalyst) proved that the water gas shift process produced an equivalent of H_2 when it was catalyzed by a biochar catalyst. About 11.86%–20.43% of H_2 was produced by Douglas fir catalytic pyrolysis using biochar. The presence of metals in the biochar catalyst, such as Fe and Cu may cause this reaction to occur (Ren et al., 2014). Similarly, one of the feasible techniques to produce hydrogen using biochar is catalytic gasification (another thermochemical method). Using biochar as a catalyst/support, the gasification of biomass was carried out for the production of H_2 by Yao et al. (2016). Approximately 64.02 vol% of H_2 production was demonstrated by cotton-char-supported Ni. The two major phases in biomass steam gasification are (1) pyrolysis, where biomass is broken down into gases, volatiles, and char, as well as (2) reforming, where gases/volatiles are reformed to generate gases like H_2 and CO in the existence of catalyst and steam (Yao et al., 2016). During the gasification of biomass, the following processes have been suggested to be included (Park et al., 2019).

$$Tars \rightarrow C + C_nH_m + gases \quad (5)$$

$$C_nH_m + H_2O \rightarrow nCO + (n + m/2)H_2 \quad (6)$$

$$C_nH_m + nCO_2 \rightarrow \frac{m}{2}H_2 + 2nCO \quad (7)$$

$$CH_4 + H_2O \rightarrow CO + 3H_2 \quad (8)$$

$$CO_2 + H_2 \rightarrow CO + H_2O \quad (9)$$

$$C + H_2O \leftrightharpoons CO + H_2 \quad (10)$$

$$C + CO_2 \leftrightharpoons 2CO \quad (11)$$

When the temperature of reforming was raised to 900 °C, the H_2 production marginally rose from 33.89 to 47.48 mg/g biomass (Yao et al., 2016). It was proposed that the endothermic characteristic of the process caused biomass decomposition (Reaction (5)) and volatile reforming (Reaction (6)) to intensify with rising temperature, leading to the generation of light gases like CH_4, H_2, CO_2, and CO. Nevertheless, at greater temperatures, char gasification (Reactions (10) and (11)) was encouraged, leading to more production of CO, while other gas amounts were decreased. As a result, the concentration of H_2 decreased from about 64 to 53 vol%. In addition, the reaction of water gas shift (Reaction (9)) was not preferred at higher temperatures and may have also played a vital role in the lower concentration of H_2 at greater temperatures. Furthermore, it was proposed that carbon gasification reactions (Reactions (10) and (11)) could be improved at greater reforming temperatures, supporting a rise in the generation of CO. Park et al. (2019) gasified high-density polyethylene (HDPE) using biochar. The highest hydrogen production was exhibited by Ni/fixed bed char, which is two times higher than the gasification of HDPE alone. Both Ni and char are attributed to the improved production of H_2 over Ni/FB char (Xiao et al., 2013). According to Reactions (5)-(9), the thermal cracking of tar and the following mechanisms of catalytic cracking can be used to confirm the greater amounts of H_2 and CO production over Ni. In addition, when biochar is employed as a support, Ni-based catalysts have an extra two reactions that are represented by Reactions (10) and (11) (Hu et al., 2018), wherein the in-situ produced coke and char during gasification are converted into H_2 and CO. As a consequence, the production of coke on Ni can be avoided in the biochar-supported catalyst, whereas coke development on biochar granules can be simulated as a catalytic function due to its improved production of H_2 upon reactivation. Thus, the possibility for improved production of hydrogen with Ni impregnation in biochar is encouraging. A further benefit of lignin-derived chars over Ni/γ-Al_2O_3 and Ni/AC was the low production amount of CO_2. Overall literature confirms biochar as a low-cost viable option for enhancing the production of H_2 from waste in the thermochemical technique.

5.1.1. Tar cracking using biochar

Based on the position of the catalyst during the process, two primary types of catalytic methods for the reduction of tar in pyrolysis and gasification techniques have been identified. The first strategy is to mix the catalyst and feedstocks directly in the reactor known as in-situ reforming, while the second strategy, known as ex-situ reforming, uses secondary tar reforming/cracking at the downstream end of the reactor (Shen and Fu, 2018). Following is a list of the primary reactions involved in tar catalytic reforming/cracking (Guo et al., 2020):

Tar thermal cracking (Reaction (12)):

$$C_mH_n\ (tar) \rightarrow C_pH_q\ (smaller\ tar) + rH_2 \quad (12)$$

Tar dry reforming (Reactions (13) and (14)):

$$C_mH_n\ (tar) + mCO_2 \rightarrow 2mCO + (n/2)H_2 \quad (13)$$

$$C_mH_n\ (tar) + (m + n/2)CO_2 \rightarrow (2m + n/2)CO + (n/2)H_2O \quad (14)$$

Tar steam reforming (Reactions (15) and (16)):

$$C_mH_n\ (tar) + mH_2O \rightarrow mCO + (m + n/2)H_2 \quad (15)$$

$$C_mH_n\ (tar) + 2mH_2O \rightarrow mCO_2 + (2m + n/2)H_2 \quad (16)$$

Table 2
Hydrogen production from different feedstock in the thermochemical technique using biochar as a catalyst.

Biochar feedstock	Conditions for biochar production	Feedstock for H_2 production	H_2 reactor condition	H_2 production	Other findings	Reference
Pyrolysis						
Biomass	• Catalyst: Ni/char • Temp: 700 °C for 2 h • Heating rate (HR): 10 °C min^{-1} • Calcination: 550 °C with 10 °C min^{-1}	Sawdust	• Temp: 700 °C • HR: 10 °C min^{-1}	~26 mmol/gbio	• At 650 °C, Ni/Char catalyst exhibited the maximum syngas yield (34.321 mmol g^{-1}). • At 300–500 °C, methane steam and tar steam reforming occurred. • Water injection, N loading, and temperature were factors for catalytic activity but not the specific surface area.	Wang et al. (2022)
Nanocellulose	• Catalyst: biochar • N_2 flow: 400 ml min^{-1} for 15 min • Power input of microwave-induced pyrolysis: 700 W for 40 min	Plastics	• Temp: 529–671 °C • Biochar to plastics feeding ratios: 1.6–4.4 • Reaction time: 15–20 min	65–92 vol%	•Gases production: 25 to 76 vol% • Methane production: 2–20 vol%	(C. Wang et al., 2021a)
Sargassum macroalgae powder	• Catalyst: biochar and Ni/SBA-15 catalyst • Temp: 700 °C for 30 min	Sargassum macroalgae	• Temp: 700 °C	3.0 and 8.54 mmol/g Sargassum for biochar and Ni/SBA-15, respectively	• H_2 production increased due to biochar's greater surface area and interconnected structure.	Taghavi et al. (2018)
Peanut shell	• Temp: 550–750 °C • HR: 5 °C min^{-1} • Modification: HCl & $MnCl_2$	Peanut shell	• Temp: 550 °C • HR: 22 °C min^{-1}	92.8%	• Biochar produced at 650 °C showed greater concentrations of H_2 and phenols. • H_2 and CH_4 were produced with the concentration of $MnCl_2$.	Chang et al. (2021)
Bamboo	• Catalyst: Zn/BC, Zr/BC, BC-ZSM-5, Zr/BC-ZSM-5 • Temp: 600 °C for 2 h • HR: 5 °C min^{-1}	Biomass	• N_2 flow: 150 mL min^{-1} for 20 min • Temp: 550 °C for 30 min	50.93 vol%	• Cleavages of C–H and aromatic C=C bonds were promoted with a biochar catalyst. • Higher production of gas products (43.10 wt%) was shown by biochar catalysts, whereas, liquid products (42.16 wt%) by ZSM-5.	Shi et al. (2022)
Corn stover	• Catalyst: Metal-doping mesoporous biochar • Temp: 800 °C for 4 h • N_2 flow: 100 mL min^{-1}	Biomass and plastics	• Biomass/plastic mass ratio: 1:1 • Temp: 600 °C for 20 s	90 NmL/$g_{feedstock}$	• Higher production of syngas (~133 NmL/$g_{feedstock}$) and H_2 was shown by Fe/C catalyst. • With 28.33 MJ kg^{-1} of HHV, biochar showed a high possibility as a solid fuel.	(R. Xu et al., 2022)
Douglas fir sawdust	• Catalyst: biochar • Power input: 700 W for 40 min • N_2 flow: 400 mL min^{-1} for 15 min	Douglas fir	• Temp: 579–721 °C • biochar to Douglas fir mass ratios: 1.6–4.4	85.32 vol%	• In comparison to non-catalytic, biochar showed two times higher H_2 production. • The biochar showed stable selectivity despite 15 cycles of reuse. • As per the predicted mechanism, water forms not only phenols but also gives an H_2 source.	(C. Wang et al., 2021b)
Gasification						
Risk husk	• Catalyst: and Ni/$ZnCl_2$-treated char, Ni/steam-treated char • Temp: 500 °C • HR: 10 °C min^{-1}	Food waste	• Temp: 800 °C • Steam flow rate: 1 ml min^{-1} for 15 min • N_2 flow rate: 50 cc min^{-1}	0.471 mol/g $_{feedstock}$•g $_{cat}$	• Due to the large amount of inherent Ca and K, and high dispersion of nickel, the higher H_2 was shown by Ni/steam-treated char. • Lower CO_2 production was shown by treated biochar. • The coke formation was prevented on Ni by the high silica content in the char.	Farooq et al. (2021a)
Sludge	• Catalyst: Ni-based sludge char • Temp: 500 °C • N_2 flow: 150 mL min^{-1} for 12 min	Sludge	• Temp: 900 °C • NiO loading rate: 20% • Steam flow rate of 1 g min^{-1}	52.22% at 0.34 m^3 kg^{-1}	• Rates of gas production: 0.76 m^3 kg^{-1} • The ratio of H_2/CO reached 1.98 with the introduction of steam, leading to increased syngas quality.	Chen et al. (2021)
Lignin	• Catalyst: Ni/FB char • Temp: 673–883 K for 3600 s	HDPE	• Temp: 1073 K • Equivalence • ratio: 0.20	~0.019 mol/0.2g of HDPE	• Biochar-based catalysts showed a greater yield of gas than Ni/AC and Ni/Al_2O_3.	Park et al. (2019)
Wheat straw and C. glomerata	• Catalyst: hydrochar • Temp: 460 °C for 20 min • Feedstock loading: 0.06 g Water loading; 6 g	Almond shell	• Temp: 460 °C • Feedstock to water ratio: 0.01 • Pressure: 270 bars	7.85 mmol g^{-1}	• With the addition of CG and WS hydrochar, the H_2 was produced by the factors of 1.48 and 1.37, respectively.	Safari et al. (2018)
Rice husk	• Catalyst: raw char, steam-activated char, KOH-activated char	Waste furniture	• Temp: 800 °C • Steam flow: 1 ml min^{-1}	• Steamed-activated char: 54.0 vol% • Raw char: 47.7 vol%	• Lower H_2 selectivity was shown by KOH-activation, which caused the demineralization of char.	Farooq et al. (2021b)

(*continued on next page*)

Table 2 (*continued*)

Biochar feedstock	Conditions for biochar production	Feedstock for H_2 production	H_2 reactor condition	H_2 production	Other findings	Reference
	• Temp: 500 °C • Steam activation: 1 ml min^{-1} at 800 °C • KOH activation of biochar: 1:1		• N_2 flow: 50 cc min^{-1}	• KOH activated char: 41.3 vol%		

In-situ catalytic cracking, which can simultaneously be completed during biomass thermochemical conversion is a useful technique for removing tar. Currently, lab-scale studies are primarily used to study the in situ catalytic efficiency of biochar-based nanotubes (BBNs). Biochar support and metal particles react with the byproducts of biomass gasification or pyrolysis when the biochar-supported catalyst is utilized for in situ catalytic tar cracking that may accelerate tar decomposition and improve the product's selectivity. Ni NPs composites supported by hydrochar produced by Gai et al. (2017). A noticeable affinity for H_2 was attained with about 78.7 g H_2/kg hydrochar, and the majority of the tar was reformed at 700–800 °C. A greater quantity of H_2 and CO_2 were produced as a result of the impregnation of Ni and Fe, whereas the production of CH_4 was suppressed. As per the findings, increasing tar conversion is a crucial aspect of raising the output of H_2. According to the investigation, greater production of H_2 resulted from increased tar conversion throughout the gasification, which is facilitated by raising the quantity of Ni salt during the one-pot hydrothermal reaction. Besides, the reaction temperature was also an important aspect of the conversion of tar. The generation of biochar support is also impacted by the reaction circumstances in the reactor during the process of in-situ catalytic reforming/cracking, resulting in variations in its specific surface area and pore structure, which can then affect the catalyst efficiency.

Another frequently employed technique for tar catalytic reforming in gasification and pyrolysis techniques is ex-situ cracking. In the context of equipment design, catalytic reforming reactions must take place in a special reaction region with catalysts in order to achieve the decomposition of tar. Therefore, typically, a reforming reactor is constructed and associated with the gasifier. This method's primary benefit is its ability to govern the reaction circumstances, including atmosphere and temperature during the tar reforming procedure. This helps to increase tar transformation and enhance the product gas selectivity. According to Shen et al. (2015), rice husk char-supported Ni NPs (RHC Ni) efficiently degraded tar produced during pyrolysis. By using 10g and 5 g of the catalyst, respectively, the efficiency of tar reforming improved to 90.5% and 99.8% at 700 °C, and about 37.5%–58.0% is the increment of gas yield with the primary components of H_2 and CO. The nascent tar components are significantly simpler to crack or reform by RHC Ni than the tertiary tar compounds of PAHs. The amount of liquid products decreased if the RHC Ni was utilized for the catalytic reforming, presumably as a result of several thermo-chemical reactions including tar steam reforming, char gasification, and water-gas-shift reaction. The BBNs are efficient and potential catalysts for tar cracking as can be observed in the study mentioned above. Mechanism of tar reforming using biochar as a catalyst is shown in Fig. 8.

5.2. Biochar as a photocatalyst in the water-splitting

Photocatalysis technology, which relies on semiconductor materials, has been widely recognized as an attractive option for converting to chemical energy from solar energy due to its affordability, eco-friendliness, and higher efficiency. Further enhancing photocatalytic activity, carbon-based materials such as biochar in combination with semiconductors had positive impacts on the activity of the catalyst. This is frequently employed in photocatalytic water splitting to produce H_2. The mechanism of photocatalytic water splitting is shown in Fig. 9. Some research on the synthesis and use of biochar as photocatalysts for H_2 production is presented in Table 3. The treatment of contaminated water and air, as well as photo-reduction of CO_2, are additional uses. The present section explores new developments in the use of semiconductor-based materials and the current material for photocatalytic applications. For a long time, conventional methods have employed semiconductor-dependent photocatalysis. For instance, bimetal sulfides like $ZnIn_2S_4$ and CdZnS (An et al., 2021; Feng et al., 2021), metal oxides like TiO_2 (Shi et al., 2021), and metal sulfides like Cds and ZnS (Kate et al., 2021; Tang et al., 2021) are employed in numerous types of semiconductor catalysts. There was considerable photocatalytic activity in these efficient and effective catalysts. However, these materials have some limitations such as difficulty in recycling, poor charge separation and low stability (such as Cds and metal oxides), excitation only in the ultraviolet

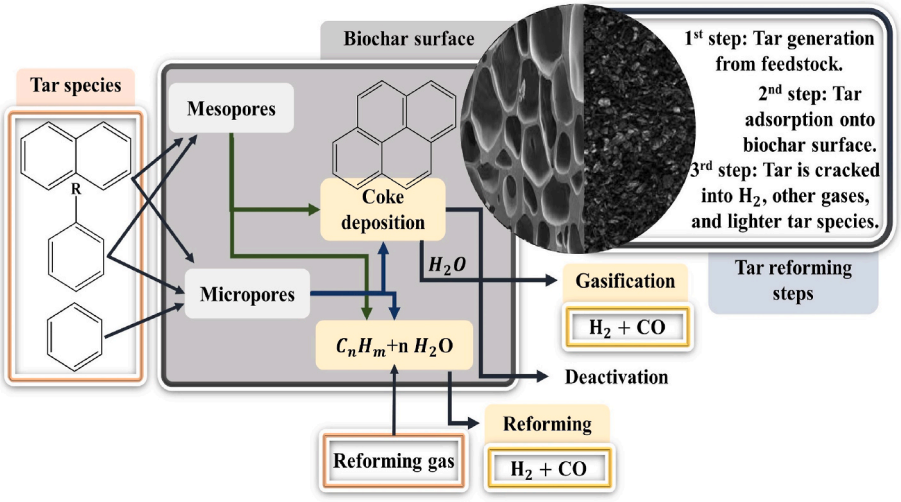

Fig. 8. Mechanism and steps of tar reforming using biochar.

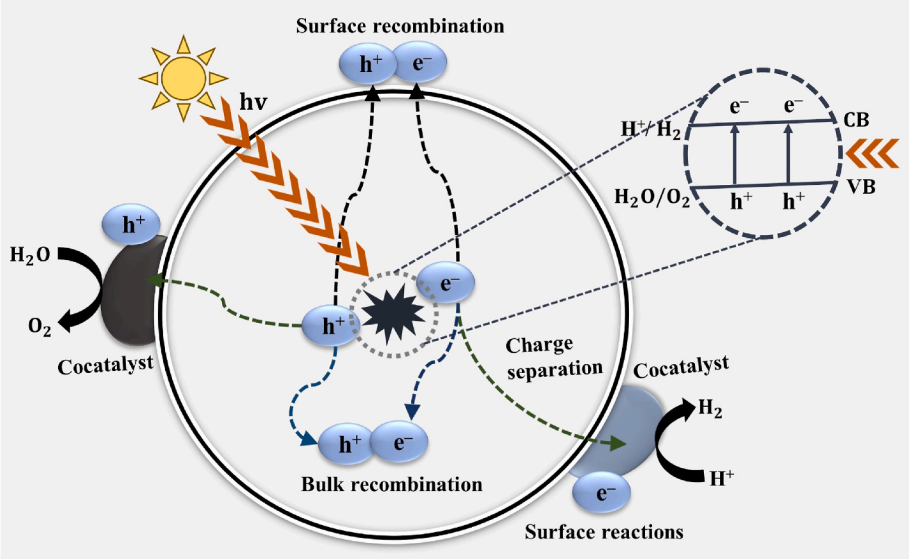

Fig. 9. Mechanism of photocatalytic water splitting.

Table 3
Production and application of biochar as photocatalysts for hydrogen production.

Biomass	Condition for biochar production	Produced catalyst	Light source	H_2 production	Reference
Bombyx mori silk fibroin	• Temp: 220 °C • Time: 12h • Reactor: hydrothermal	–	300 W Xe lamp	30.12 μmol $h^{-1}g^{-1}$	(Q. Wang et al., 2020)
Leaves of Japanese raisin tree	• Temp: 200 °C • Time: 12h • Reactor: hydrothermal	–	Visible light	5.71 mmol h^{-1} g^{-1}	(M. Xu et al., 2022)
Strawberries and Bamboo	• Carbonization and Acid treatment	–	Halogen (630 nm) light	518 μmol h^{-1} g^{-1}	Sofi'i et al. (2020)
Coconut shell	• Temp: 600 °C (carbonized) • Time: 2h	Pt/CdS/BC	Xe lamp (300 W, $\lambda > 420$ nm)	1679.5 μmol h^{-1}	Zha et al. (2016)
Sawdust	• Temp: 800 °C • Gasifying agent: CO_2 • Reactor: gasification	Au–TiO_2/BC	UV light	34 mmol	Jiang et al. (2018)
	• Temp: 1000 °C • Time: 1 h in N_2 environment • Reactor: pyrolysis	Au–TiO_2/BC	Visible light	23 mmol	
Pythium oligandrum	• Temp: 600 °C (calcined) for the time of 1 h	–	Visible light	600 μmol	Zheng et al. (2021)
Poplar catkins	• Calcined: 800 °C • Time: 2 h • Heating rate: 5 °C min^{-1}	–	Xe lamp (300 W, $\lambda = 420$ nm)	5367 μmol h^{-1} g^{-1}	Xiang et al. (2019)
Pear	• Reactor: hydrothermal carbonization	N-fGNS	Visible light	1380 μmol h^{-1} g^{-1}	Das et al. (2020)
Natural plane tree	• Temp: 900 °C for the time of 5 h in an Ar environment	–	Visible	94.4 μmol h^{-1} g^{-1}	S. Wang et al. (2019)
			Under UV, Xe lamp (300 W, $\lambda = 420$ nm)	5.427 mmol h^{-1} g^{-1}	
Corn stalks	• Temp: 500 °C for the time of 2 h in N_2 and CO_2 environment • Reactor: pyrolysis	BC/$ZnFe_2O_4$	Xe lamp (300 W, $\lambda > 420$ nm)	1219 μmol g^{-1} h^{-1}	Chen et al. (2019)
Sewage Sludge	• Temp: 700 °C for 15 min • Reactor: pyrolysis	Fe_3O_4/BC	Visible light (300 W, λ 420 nm)	3845 mmol g^{-1}	Norouzi et al. (2019)

region (such as ZnS and TiO_2), and Cd-based catalyst toxicity.

The primary limitations are photo-corrosion effects (such as Zns and CdS), homogeneous nature, and the higher bandgap (such as TiO_2) for their application. The use of co-catalyzed homogeneous and heterogeneous catalysts as well as heterogeneous catalysts alone are examples of the efforts, which have been implemented to address these limitations (Figueiredo, 2013). Utilizing various techniques such as subsequent functionalization strategy, and thermal or photo-deposition chemical post-treatment methods, the carbon-based substance can perform as a useful support/co-catalyst for the single metal atoms or heteroatoms accumulation on semiconductor-based photocatalytic. To create depositional sites for hetero/metal atoms, it can be used to modify the structures of the surface and add different functional groups on it, such as -NH_2, -COOH, and -OH. By reducing the movement of metal crystallites, they also prevent metal aggregation (Matsagar et al., 2021). However, the metal deposition and dispersion on the biochar have a major effect on the catalytic activity. Biochar plays a useful role in photoactive and photocatalyst heterojunctions when changed with semiconductors. The advantages such as reducing the bandgap energy, increasing the efficiency of charge separation, acting as an electron sink,

as well as enhancing the shuttling electrons, active sites number, and surface area make biochar a suitable supporting substance for the deposition of nanoparticles (Mian and Liu, 2018; Shan et al., 2020). Absorbing light of the appropriate energy, which relies on the semiconductor's bandgap excites electron-hole pairs when solar radiation strikes a composite semiconductor with a biochar modification. Electrons that are excited are moved to the valence band from the conduction band and then to a narrow bandgap of biochar; throughout this transfer process, the electron settling was noticed. These successfully caused the water splitting, forming H_2 (Saleem et al., 2020). Different biomass was used by Norouzi et al. (2019) to synthesize the biochar as a catalyst. Afterward, the biochar was loaded with Iron oxide, and under visible light irradiation, photocatalytic production of H_2 was examined. Greater catalytic activity (ca. 4162 mmol/g of H_2 after 3 h light irradiation) was observed after rice husk-derived biochar was loaded with iron oxide metal, which increased the surface area. The findings showed that electrons were moving from Fe_3O_4 to biochar. Biochar was sensitizing Fe_3O_4's huge band gap energy, and iron-based biochar had higher levels of light absorption. This study proposed biochar from sludge as a renewable and biomass-based substitute for traditional metal-based photocatalysts, as well as an innovative and effective path approaching biochar-based composites for visible light photocatalysis. The biochar was produced by Matos (2016) and activated with different techniques such as chemical activation using H_3PO_4 and $ZnCl_2$, as well as gasification with N_2 and CO_2. Higher production of H_2 (i.e., 23 mmol and 34 mmol for 4 h visible light and ultraviolet irradiation) was confirmed using Au–TiO_2/BC (CO_2-activated biochar). When exposed to visible light, $ZnFe_2O_4$ catalytic composites supported by biochar produced from corn stalks have significantly more photocatalytic H_2 than $ZnFe_2O_4$ alone. By using BC/$ZnFe_2O_4$ catalysts with an optimized mass ratio of 5:1, the rate of H_2 generation improved and was about six times higher (1219 μmol $g^{-1}h^{-1}$) in comparison to $ZnFe_2O_4$ alone. Biochar served as an electron mediator in this composite system, effectively promoting electron-hole separation to increase the rate of the photocatalytic process. Additionally, triethanolamine (TEOA) and Eosin Y demonstrated improved photocatalytic efficacy (Chen et al., 2019).

Biochar produced from a natural plane tree was utilized to produce tri-level linked porous carbon supported by TiO_2 (TiO_2/C). Under visible light and UV excitation, the TiO_2/C catalyst's photocatalytic water-splitting efficiency with various co-catalysts was investigated, whereas, in this system, methanol is utilized as a scavenger. Under visible light and UV irradiation, the Pt-Mo_2C loaded TiO_2/C nanocomposites demonstrate effective photocatalytic hydrogen production of 94.4 4 μmol g^{-1} h^{-1} (vis) and 5.427 mmol h^{-1} g^{-1}, respectively (H. Wang et al., 2019). For photocatalytic water splitting, pythium oligandrum biomass-derived carbon (POC) was synthesized in a single environmentally friendly process. Roughly 600 μmol of H_2 was produced using Pt co-catalyzed POC in 2 h. Eosin Y was utilized as an electron transporter in this system. Eosin Y species accelerated the catalyst surfaces and the electrons could get into POC/Pt. As a result of the diffused electrons' ability to move with the POC surface and become captured by Pt, H^+ is reduced to produce H_2 (Zheng et al., 2021).

5.3. *Biochar as a catalyst in dark fermentation*

A sustainable substitute technique "biological hydrogen generation" utilizes renewable resources as substrates, i.e., organic waste (Kumar et al., 2021; Liu et al., 2019). The generation of biohydrogen from complicated organic waste could be improved by the use of biochar. The utilization of biochar in dark fermentation systems to encourage the co-production of hydrogen and methane, as well as the biochar's promoting mechanisms were reported (Sunyoto et al., 2017; Yao et al., 2016). Biochar was found to considerably improve the yield and rate of H_2 generation by up to 41% and 26%. The encouragement of H_2 generation was attributed to the temporary nutrient supply, microbial attachment support, and pH buffer capacity. Incorporating biochar into the biohydrogen method serves as a cell carrier, promotes the electron mobility and growth of biofilms, as well as serves as an effective conductive substance. The growth of H_2 is strongly connected to improved extracellular electron transfer (EET). Biochar improves electron transport by increasing electroactive microorganisms and substituting the conductive secretions involved in EET (Bu et al., 2021). The mechanism of biochar utilization in dark fermentation for hydrogen production is shown in Fig. 10.

The production of biochar and application in dark fermentation for hydrogen production is presented in Table 4. Using food waste as a substrate, Sunyoto et al. (2017) investigated biochar's impact on the generation of H_2 under various pH circumstances. Adding 10 g L^{-1} of biochar led to the highest H_2 output (1475 mL L^{-1}) and H_2 production rate (HPR) (820 mL L^{-1}) at a pH of 6. However, without the use of biochar, low generation of H_2 (production: 1044 mL L^{-1}, HPR: 651 mL L^{-1} at pH 6) was produced, demonstrating the biochar's capacity to support provisional availability of nutrients, biofilm developments, and buffering conditions. Moreover, the biochar's ability to adsorb ammonium ions is suppressed by its inclusion in the biohydrogen process (Chu et al., 2013). Additionally, biochar preserves the culture's stability, facilitates buffering conditions, and shortens the initial lag period while providing a substrate for the growth of microbes and metabolism (Bharathiraja et al., 2016). The maximum generation of H_2 (i.e., 204 mL/g glucose) was discovered at the amount of 600 mg/L biochar, according to Zhang et al. (2017), and also showed a rise in the H_2 generation with changing the biochar concentrations and Fe^{2+}. Fe^{2+} particularly encourages the activity of hydrogenase enzyme and enhances the benefits of biochar that have already been noted.

The hydrogen-producing bacteria (HPB), gene expression, medium pH value, metabolite accumulation, and routes, as well as the lag period in the bioprocess, are influenced by the concentration of biochar (Zhang et al., 2017). Moreover, certain bacteria can live deep into biochar's pore channels, which is exceptionally advantageous for the development of hydrogenogenic zones in the bioprocess systems. Further, even in the early stages of H_2 development, a large number of HPBs are already abundant in the vicinity of biochar (Cooney et al., 2016). These microbes' preference for the biochar surface could have the following reasonable reasons: (1) porous biochar encourages the formation of biofilms, (2) porous biochar increases the efficiency of direct electron or H_2 transfer, and (3) importantly, by changing the pH of the solution, alkali biochar can function as a buffer. It might also be stated that biochar serves just as a medium for the growth of cells and microbial attachment, which raises the concentration of biomass. Irrespective of the type of biomass, Wang et al. (2018) observed that biochar utilization led to maximum generation production of H_2 and a short lag time. It could be due to biochar's greater electrical conductivity, porosity, and other chemical and physical properties. It is considered that biochar's specific surface area promotes microbial adhesion and increases microbial biomass. Using Mg- and Ca-saturated resins along with phosphate-rich biochar, a hybrid dark-photo bioreactor was used to study H_2 generation (Rezaeitavabe et al., 2020).

The generation rate of H_2 was enhanced, i.e., from about 101 to 164 mL H_2 g^{-1} VS with the introduction of the Mg- and Ca-saturated resins and it also affected the pH of the system. Following this, the introduction of phosphate-rich biochar and saturated resin (5 g L^{-1}) enhanced the metabolic activity and led to the highest H_2 yield (197 mL/g VS) and productivity (3130 mL), which accounted for 94% of the total H_2 generated. The method was referred to as mixed photo and dark fermentation, and it was discovered that adding biochar considerably raised the H_2 production with the highest productivity rising 12 mol H_2 mol^{-1} glucose from 4 mol H_2 mol^{-1} glucose to. In a circular process, the remaining biochar from the generation of biohydrogen was also utilized to increase the H_2 output. Additionally, with 5.7 mL H_2 g^{-1} substrate/h, the residual biochar (15 g L^{-1}) produced from dark fermentation of cornstalk generates 286 mL H_2 g^{-1} (Zhao et al., 2021a).

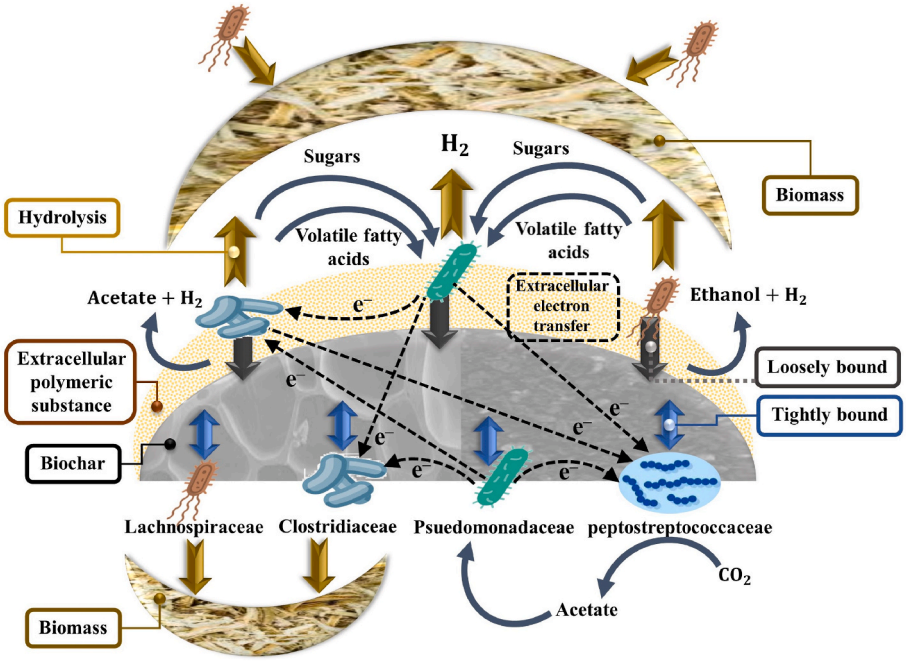

Fig. 10. Schematic diagram of biochar utilization in dark fermentation for hydrogen production by creating a synergistic impact and allowing functioning bacteria to transfer electrons for syntrophic metabolism. Adapted from (Bu et al., 2021), with permission from Elsevier.

Table 4
Production of biochar and application in dark fermentation for hydrogen production.

Biochar feedstock	Temperature (°C) for biochar production	Substrate	Inoculum	Other factors	H_2 production without biochar	H_2 production with biochar	Reference
Fallen leaves	600	Sewage sludge	Activated sewage sludge	• Biochar usage: 10 g L^{-1}	28.6 mM	119.3 mM	Bu et al. (2021)
Pinewood	900 600	Food waste	Sewage sludge	• Pretreatment temp: 95 °C for 30 min • Biochar usage: 15 g L^{-1}	610 mL L^{-1}	1154 mL L^{-1} 957 mL L^{-1}	Sugiarto et al. (2021)
Sugarcane bagasse	300	Glucose	*E. harbinense* Yuan-3	• Biochar usage: 3 g L^{-1}	106.5 mL	124.8 mL	Li et al. (2021)
Woody biomass	500	Municipal solid waste (organic fraction)	*Enterobacter aerogenes* and *E.Coli*	• Biochar usage: 12.5 g L^{-1}	0.60 L L^{-1} substrate	2.58 L L^{-1} substrate	Sharma and Melkania (2017)
Rice straw	700	Glucose	*Ethanoligenens harbinense Yuan-3*	• Biochar usage: 3 g L^{-1}	1.11 mol mol^{-1}	2.36 mol mol^{-1}	(W. Li et al., 2020)
Sewage sludge	500	Synthetic food waste	*R. sphaeroides* and *C. acetobutylicum*	• Biochar usage: 0.5 g L^{-1}	102.00 mL g^{-1} VS	197.15 mL g^{-1} VS	Rezaeitavabe et al. (2020)
Corn-bran residue	600	Glucose	Sewage sludge	• Pre-treatment temp: 85 °C for 30 min • Biochar usage: 600 mg L^{-1}	–	204.0 mL g^{-1}	Zhang et al. (2017)
Residue cornstalk	300	Cornstalk hydrolysate	*Clostridium* sp. T2	• Biochar usage: 10 g L^{-1}	2364 mL L^{-1}	3215 mL L^{-1}	Zhao et al. (2020)
Sawdust	500	Grass biomass	Anaerobic Sludge	• Biochar usage: 600 mg L^{-1}	26.6 mL g^{-1} dry grass	30.9 mL g^{-1} dry grass	Yang and Wang (2019)
Residue cornstalk	500	Pretreated Cornstalk	*T. thermosaccharolyticum M18*	• Biochar usage: 15 g L^{-1}	–	5.7 mL g^{-1} substrate h^{-1}	Zhao et al. (2021a)
Sewage sludge Sawdust Wheat bran	700 700 700	Activated sludge and food waste	Brewery Waste Anaerobic Sludge	• Biochar usage: 10 g L^{-1}	72 ± 3 mL g^{-1} VS	73 ± 3 mL g^{-1} VS 81 ± 3 mL g^{-1} VS 81 ± 2 mL g^{-1} VS	Wang et al. (2018)
Pine Sawdust	650	Food Waste	Anaerobic Sludge	• Biochar usage: 10 g L^{-1}	651 ± 7 mL l^{-1} day^{-1}	820.6 ± 81 mL l^{-1} day	Sunyoto et al. (2017)

5.4. Biochar as a catalyst for methane steam reforming

The existence of oxygen-comprising functional groups on the surface of biochar and biochar's huge surface area promotes oxidation reaction, its catalyst performance is attractive for the gaseous reaction (Nguyen et al., 2020). Catalytic steam reforming of methane using metal-doped biochar is shown in Fig. 11. The investigation of microwave (MW) assisted dry reforming of methane (DRM) over biochar produced by biomass pyrolysis at 800 °C and volumetric hourly space velocity (VHSV) of 0.166 L g^{-1} h^{-1} originated by Domínguez et al. (2007). They discovered that over the potassium biochar catalyst, two reactions (i) decomposition or cracking of CH_4 into C and H_2, as well as (ii) CO_2 adsorption dissociative then reduction to CO occurred simultaneously. In combination with DRM, the first study of steam reforming of methane (SRM) over biochar under conventional heating and irradiation of MW at different temperatures of 600–800 °C was conducted by Li et al. (2016). The input flow rate includes steam and CO_2 mixture (30 mL min^{-1}), as well as CH_4 (30 mL min^{-1}). Three variables were identified as the causes of this increased conversion when exposed to MW radiation: (i) the development of hotspots (ii) biochar's high MW absorption and (iii) lower the reforming reactions' apparent activation energy by non-thermal effects of MW. With improvement in H_2 selectivity after CH_4 transformation, Super-dry reforming (SDR) was predicted to be more effective than DRM at increasing the H_2 to CO ratio. SDR and DRM assisted by MW over pristine biochar and biochar-Ni/Al_2O_3 were investigated by Li et al. (2017). SDR had a CH_4 transformation and H_2 selectivity that was about 4.5% greater than DRM's. The most effective efficiency was shown by a 10% weight ratio of biochar with carbon to Ni.

The findings showed that combined reforming can effectively retain the stability of Ni/biochar while also favoring the transformation of CH_4. The first reason for this modification is to differentiate between dry and steam reformation. This is also because the addition of H_2O accelerates the elimination of carbon deposits. In addition, BC-H_2O was combined by Li et al. (2018) with various compounds, including MgO, CaO, K_2CO_3, Na_2CO_3, and synthetic Ni catalysts. The most prominent improvement in CO_2 and CH_4 conversions, from about 81% to 87%, was obtained when Ni was added to BC-H_2O, which can be explained by the fact that Ni has greater catalytic activity than the alkaline earth metal. They found that concerning reforming effectiveness, SDR is more advantageous for the generation of syngas than DRM and SRM as shown by higher production of H_2 and CH_4 conversion for the former. Despite this, biochar deactivation caused the efficiency to steadily decline to 47% after 180 min of continuous DRM.

Their SDR assisted by MW needed a power input of 4.14 kW h^{-1} to generate 1 m^3 of H_2, which is more than that stated in the study of Fidalgo and Menéndez (2012) and required a power input of 1.2 kW h^{-1} to accomplish the same accomplishment over a catalyst made of activated carbon and Ni. For MW-assisted DRM, L. Li et al., 2019 investigated the catalytic efficacy of a single biochar and its mixture with Fe_2O_3. When compared to its mixture with Fe_2O_3, they discovered that a single biochar's catalytic activity was significantly reduced. Moreover, 98% CO_2 and 95% CH_4 conversions at 800 °C over a Fe-biochar catalyst (10 wt% Fe) can yield an H_2 to CO ratio that is almost 1. Because of the existence of a reducing agent, namely H_2, in the gaseous phase, extremely active FeO sites for DRM were formed on the Fe-char catalyst, which was accountable for its distinct catalytic activity. In addition, the existence of Fe_2O_3 caused biochar to emit volatile substances that enlarge the surface area necessary for adsorbed reactants' dissociation, such as CO_2 and CH_4, increasing the reaction efficiency. Since carbon-based catalysts have such effective MW absorption capabilities, they have been widely used in this field. However, carbon's disadvantage is that it is bound to be consumed by reactions with co-reactants like H_2O, CO_2, and O_2. The intense MW reflection of metals has caused scientists to pay much less consideration to metal-based catalysts.

6. Conclusion

This review paper has primarily focused on the catalytic performance of biochar for hydrogen production using different techniques. The application of biochar as a catalyst in various techniques, such as thermochemical techniques (pyrolysis or gasification), photocatalytic water splitting, dark fermentation, and methane steam reforming, has shown promising prospects. Biochar can enhance the yield of hydrogen, reduce GHG emissions, and provide an eco-friendly alternative to conventional catalysts. The application of biochar to the feedstock or introducing it as a separate catalyst bed can ameliorate the production of hydrogen in thermochemical processes, whereas biochar-based photocatalysts can enhance the efficiency of photocatalytic water splitting. In dark fermentation, biochar can improve the organic matter degradation, which leads to enhanced biogas yield. In methane steam reforming, it can act as a catalyst support to improve the performance of conventional catalysts. The mechanism will also be beneficial to evaluate the long-term stability of biochar as a catalyst. Overall, this review shows that biochar is a promising catalyst for various applications for hydrogen-rich syngas. There is also a need for further studies to explore its potential as a catalyst to analyze its long-term environmental and

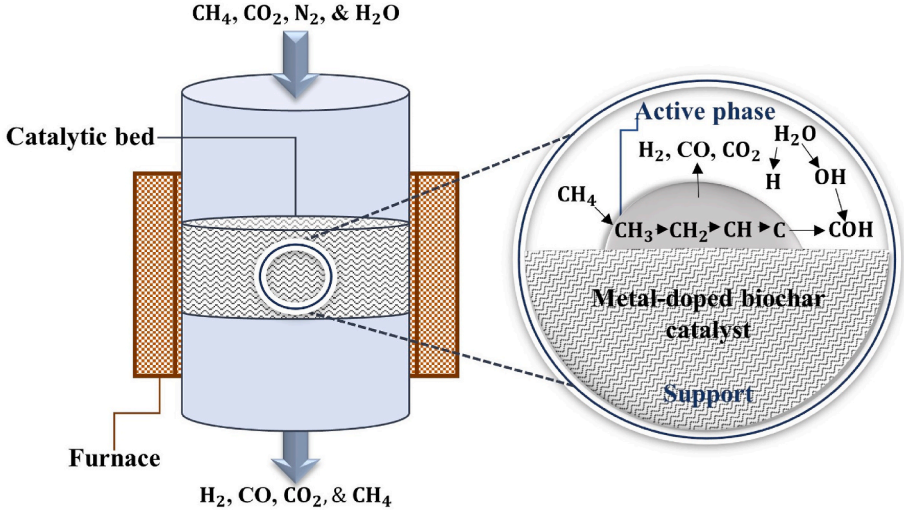

Fig. 11. Catalytic steam reforming of methane using metal-doped biochar.

economic impacts. However, the existing information suggests that biochar can play an important role in the production of sustainable energy.

Funding

The authors declare that no funds, grants, or other support were received during the preparation of this manuscript.

CRediT authorship contribution statement

Rahul Mishra: Writing – original draft, Writing – review & editing, Investigation, Formal analysis, Data curation, Conceptualization. **Chi-Min Shu:** Writing – review & editing, Supervision. **Hwai Chyuan Ong:** Writing – review & editing, Supervision. **Anjani R.K. Gollakota:** Writing – review & editing. **Sunil Kumar:** Writing – review & editing.

Declaration of competing interest

The authors declare that they have no known competing financial interests or personal relationships that could have appeared to influence the work reported in this paper.

Data availability

Data will be made available on request.

Acknowledgments

The authors would like to acknowledge the support of Sunway University, Malaysia under Research Accelerator Grant Scheme (GRTIN-RAG-DEN-07-2024) and National Yunlin University of Science and Technology, Taiwan.

References

Adeniyi, A.G., Ighalo, J.O., Onifade, D.V., 2020. Biochar from the thermochemical conversion of orange (citrus sinensis) peel and albedo: product quality and potential applications. Chemistry Africa 3, 439–448. https://doi.org/10.1007/s42250-020-00119-6.

Ahmad, M., Lee, S.S., Rajapaksha, A.U., Vithanage, M., Zhang, M., Cho, J.S., Lee, S.-E., Ok, Y.S., 2013. Trichloroethylene adsorption by pine needle biochars produced at various pyrolysis temperatures. Bioresour. Technol. 143, 615–622. https://doi.org/10.1016/j.biortech.2013.06.033.

Ahmed, I., Zia, M.A., Afzal, H., Ahmed, S., Ahmad, M., Akram, Z., Sher, F., Iqbal, H.M.N., 2021. Socio-economic and environmental impacts of biomass valorisation: a strategic drive for sustainable bioeconomy. Sustainability 13, 4200. https://doi.org/10.3390/su13084200.

Al-Rumaihi, A., Shahbaz, M., Mckay, G., Mackey, H., Al-Ansari, T., 2022. A review of pyrolysis technologies and feedstock: a blending approach for plastic and biomass towards optimum biochar yield. Renew. Sustain. Energy Rev. 167, 112715. https://doi.org/10.1016/j.rser.2022.112715.

Alvarez, J., Amutio, M., Lopez, G., Barbarias, I., Bilbao, J., Olazar, M., 2015. Sewage sludge valorization by flash pyrolysis in a conical spouted bed reactor. Chem. Eng. J. 273, 173–183. https://doi.org/10.1016/j.cej.2015.03.047.

An, H., Lv, Z., Zhang, K., Deng, C., Wang, H., Xu, Z., Wang, M., Yin, Z., 2021. Plasmonic coupling enhancement of core-shell Au@Pt assemblies on ZnIn2S4 nanosheets towards photocatalytic H2 production. Appl. Surf. Sci. 536, 147934. https://doi.org/10.1016/j.apsusc.2020.147934.

Asadullah, M., Ito, S., Kunimori, K., Yamada, M., Tomishige, K., 2002. Biomass gasification to hydrogen and syngas at low temperature: novel catalytic system using fluidized-bed reactor. J. Catal. 208, 255–259. https://doi.org/10.1006/jcat.2002.3575.

Balajii, M., Niju, S., 2019. Biochar-derived heterogeneous catalysts for biodiesel production. Environ. Chem. Lett. 17, 1447–1469. https://doi.org/10.1007/s10311-019-00885-x.

Bhandari, P.N., Kumar, A., Bellmer, D.D., Huhnke, R.L., 2014. Synthesis and evaluation of biochar-derived catalysts for removal of toluene (model tar) from biomass-generated producer gas. Renew. Energy 66, 346–353. https://doi.org/10.1016/j.renene.2013.12.017.

Bharathiraja, B., Sudharsanaa, T., Bharghavi, A., Jayamuthunagai, J., Praveenkumar, R., 2016. Biohydrogen and Biogas – an overview on feedstocks and enhancement process. Fuel 185, 810–828. https://doi.org/10.1016/j.fuel.2016.08.030.

Bhatia, S.K., Gurav, R., Choi, T.-R., Kim, H.J., Yang, S.-Y., Song, H.-S., Park, J.Y., Park, Y.-L., Han, Y.-H., Choi, Y.-K., Kim, S.-H., Yoon, J.-J., Yang, Y.-H., 2020. Conversion of waste cooking oil into biodiesel using heterogenous catalyst derived from cork biochar. Bioresour. Technol. 302, 122872. https://doi.org/10.1016/j.biortech.2020.122872.

Bhavani, P., Praveen Kumar, D., Jeong, S., Kim, E.H., Park, H., Hong, S., Gopannagari, M., Amaranatha Reddy, D., Song, J.K., Kim, T.K., 2018. Multidirectional-charge-transfer urchin-type Mo-doped $W_{18}O_{49}$ nanostructures on CdS nanorods for enhanced photocatalytic hydrogen evolution. Catal. Sci. Technol. 8, 1880–1891. https://doi.org/10.1039/C7CY02162C.

Bielan, Z., Siuzdak, K., 2023. Transition metal oxides in solar-to-hydrogen conversion. In: Materials for Hydrogen Production, Conversion, and Storage. Wiley, pp. 1–39. https://doi.org/10.1002/9781119829584.ch1.

Brewer, C.E., Schmidt-Rohr, K., Satrio, J.A., Brown, R.C., 2009. Characterization of biochar from fast pyrolysis and gasification systems. Environ. Prog. Sustain. Energy 28, 386–396. https://doi.org/10.1002/ep.10378.

Bu, J., Wei, H.-L., Wang, Y.-T., Cheng, J.-R., Zhu, M.-J., 2021. Biochar boosts dark fermentative H2 production from sugarcane bagasse by selective enrichment/colonization of functional bacteria and enhancing extracellular electron transfer. Water Res. 202, 117440. https://doi.org/10.1016/j.watres.2021.117440.

Campos, P., De la Rosa, J.M., 2020. Assessing the effects of biochar on the immobilization of trace elements and plant development in a naturally contaminated soil. Sustainability 12, 6025. https://doi.org/10.3390/su12156025.

Cao, B., Yuan, J., Jiang, D., Wang, S., Barati, B., Hu, Y., Yuan, C., Gong, X., Wang, Q., 2021. Seaweed-derived biochar with multiple active sites as a heterogeneous catalyst for converting macroalgae into acid-free biooil containing abundant ester and sugar substances. Fuel 285, 119164. https://doi.org/10.1016/j.fuel.2020.119164.

Cao, X., Sun, S., Sun, R., 2017. Application of biochar-based catalysts in biomass upgrading: a review. RSC Adv. 7, 48793–48805. https://doi.org/10.1039/C7RA09307A.

Cao, Y., Mao, S., Li, M., Chen, Y., Wang, Y., 2017. Metal/porous carbon composites for heterogeneous catalysis: old catalysts with improved performance promoted by N-doping. ACS Catal. 7, 8090–8112. https://doi.org/10.1021/acscatal.7b02335.

Cay, H., Duman, G., Yanik, J., 2019. Two-step gasification of biochar for hydrogen-rich gas production: effect of the biochar type and catalyst. Energy & Fuels 33, 7398–7405. https://doi.org/10.1021/acs.energyfuels.9b01354.

Cha, J.S., Choi, J.-C., Ko, J.H., Park, Y.-K., Park, S.H., Jeong, K.-E., Kim, S.-S., Jeon, J.-K., 2010. The low-temperature SCR of NO over rice straw and sewage sludge derived char. Chem. Eng. J. 156, 321–327. https://doi.org/10.1016/j.cej.2009.10.027.

Cha, J.S., Park, S.H., Jung, S.-C., Ryu, C., Jeon, J.-K., Shin, M.-C., Park, Y.-K., 2016. Production and utilization of biochar: a review. J. Ind. Eng. Chem. 40, 1–15. https://doi.org/10.1016/j.jiec.2016.06.002.

Chakraborty, P., Singh, S.D., Gorai, I., Singh, D., Rahman, W.-U., Halder, G., 2020. Explication of physically and chemically treated date stone biochar for sorptive remotion of ibuprofen from aqueous solution. J. Water Proc. Eng. 33, 101022. https://doi.org/10.1016/j.jwpe.2019.101022.

Chang, C., Liu, Z., Li, P., Wang, X., Song, J., Fang, S., Pang, S., 2021. Study on products characteristics from catalytic fast pyrolysis of biomass based on the effects of modified biochars. Energy 229, 120818. https://doi.org/10.1016/j.energy.2021.120818.

Chen, A., Hu, R., Han, R., Wei, X., Tian, Z., Chen, L., 2021. The production of hydrogen-rich gas from sludge steam gasification catalyzed by Ni-based sludge char prepared with mechanical ball-milling. J. Energy Inst. 99, 21–30. https://doi.org/10.1016/j.joei.2021.07.015.

Chen, D., Wang, X., Zhang, X., Yang, Y., Xu, Y., Qian, G., 2019. Facile fabrication of mesoporous biochar/ZnFe2O4 composite with enhanced visible-light photocatalytic hydrogen evolution. Int. J. Hydrogen Energy 44, 19967–19977. https://doi.org/10.1016/j.ijhydene.2019.06.021.

Chi, N.T.L., Anto, S., Ahamed, T.S., Kumar, S.S., Shanmugam, S., Samuel, M.S., Mathimani, T., Brindhadevi, K., Pugazhendhi, A., 2021. A review on biochar production techniques and biochar based catalyst for biofuel production from algae. Fuel 287, 119411. https://doi.org/10.1016/j.fuel.2020.119411.

Chu, C.-Y., Tung, L., Lin, C.-Y., 2013. Effect of substrate concentration and pH on biohydrogen production kinetics from food industry wastewater by mixed culture. Int. J. Hydrogen Energy 38, 15849–15855. https://doi.org/10.1016/j.ijhydene.2013.07.088.

Cooney, M.J., Lewis, K., Harris, K., Zhang, Q., Yan, T., 2016. Start up performance of biochar packed bed anaerobic digesters. J. Water Proc. Eng. 9, e7–e13. https://doi.org/10.1016/j.jwpe.2014.12.004.

Cui, X., Lu, M., Khan, M.B., Lai, C., Yang, X., He, Z., Chen, G., Yan, B., 2020. Hydrothermal carbonization of different wetland biomass wastes: phosphorus reclamation and hydrochar production. Waste Management 102, 106–113. https://doi.org/10.1016/j.wasman.2019.10.034.

Das, G.S., Bhatnagar, A., Yli-Pirilä, P., Tripathi, K.M., Kim, T., 2020. Sustainable nitrogen-doped functionalized graphene nanosheets for visible-light-induced photocatalytic water splitting. Chem. Commun. 56, 6953–6956. https://doi.org/10.1039/D0CC01365J.

Dehkhoda, A.M., West, A.H., Ellis, N., 2010. Biochar based solid acid catalyst for biodiesel production. Appl. Catal. Gen. 382, 197–204. https://doi.org/10.1016/j.apcata.2010.04.051.

Deng, L., Zhang, Y., Wang, Y., Yuan, H., Chen, Y., Wu, Y., 2021. In situ N-, P- and Ca-codoped biochar derived from animal bones to boost the electrocatalytic hydrogen evolution reaction. Resour. Conserv. Recycl. 170, 105568. https://doi.org/10.1016/j.resconrec.2021.105568.

Díaz, L., Rodríguez, V.D., González-Rodríguez, M., Rodríguez-Castellón, E., Algarra, M., Núñez, P., Moretti, E., 2021. M/TiO_2 (M = Fe, Co, Ni, Cu, Zn) catalysts for

photocatalytic hydrogen production under UV and visible light irradiation. Inorg. Chem. Front. 8, 3491–3500. https://doi.org/10.1039/D0QI01311K.
Ding, D., Yang, S., Qian, X., Chen, L., Cai, T., 2020. Nitrogen-doping positively whilst sulfur-doping negatively affect the catalytic activity of biochar for the degradation of organic contaminant. Appl. Catal., B 263, 118348. https://doi.org/10.1016/j.apcatb.2019.118348.
Domínguez, A., Fernández, Y., Fidalgo, B., Pis, J.J., Menéndez, J.A., 2007. Biogas to syngas by microwave-assisted dry reforming in the presence of char. Energy & Fuels 21, 2066–2071. https://doi.org/10.1021/ef070101j.
Farooq, A., Jang, S.-H., Lee, S.H., Jung, S.-C., Rhee, G.H., Jeon, B.-H., Park, Y.-K., 2021a. Catalytic steam gasification of food waste using Ni-loaded rice husk derived biochar for hydrogen production. Chemosphere 280, 130671. https://doi.org/10.1016/j.chemosphere.2021.130671.
Farooq, A., Rhee, G.H., Lee, I.-H., Khan, M.A., Lee, S.H., Jung, S.-C., Jeon, B.-H., Chen, W.-H., Park, Y.-K., 2021b. Waste furniture gasification using rice husk based char catalysts for enhanced hydrogen generation. Bioresour. Technol. 341, 125813. https://doi.org/10.1016/j.biortech.2021.125813.
Feng, C., Chen, Z., Jing, J., Sun, M., Tian, J., Lu, G., Ma, L., Li, X., Hou, J., 2021. Significantly enhanced photocatalytic hydrogen production performance of g-C3N4/CNTs/CdZnS with carbon nanotubes as the electron mediators. J. Mater. Sci. Technol. 80, 75–83. https://doi.org/10.1016/j.jmst.2020.11.047.
Fidalgo, B., Menéndez, J.A., 2012. Study of energy consumption in a laboratory pilot plant for the microwave-assisted CO2 reforming of CH4. Fuel Process. Technol. 95, 55–61. https://doi.org/10.1016/j.fuproc.2011.11.012.
Figueiredo, J.L., 2013. Functionalization of porous carbons for catalytic applications. J Mater Chem A Mater 1, 9351. https://doi.org/10.1039/c3ta10876g.
Funke, A., Ziegler, F., 2010. Hydrothermal carbonization of biomass: a summary and discussion of chemical mechanisms for process engineering. Biofuels, Bioproducts and Biorefining 4, 160–177. https://doi.org/10.1002/bbb.198.
Gai, C., Zhang, F., Guo, Y., Peng, N., Liu, T., Lang, Q., Xia, Y., Liu, Z., 2017. Hydrochar-supported, *in situ* -generated nickel nanoparticles for sorption-enhanced catalytic gasification of sewage sludge. ACS Sustain Chem Eng 5, 7613–7622. https://doi.org/10.1021/acssuschemeng.7b00924.
González, J.F., Román, S., Encinar, J.M., Martínez, G., 2009. Pyrolysis of various biomass residues and char utilization for the production of activated carbons. J. Anal. Appl. Pyrolysis 85, 134–141. https://doi.org/10.1016/j.jaap.2008.11.035.
Guo, F., Jia, X., Liang, S., Zhou, N., Chen, P., Ruan, R., 2020. Development of biochar-based nanocatalysts for tar cracking/reforming during biomass pyrolysis and gasification. Bioresour. Technol. 298, 122263. https://doi.org/10.1016/j.biortech.2019.122263.
Hernández, J.J., Saffe, A., Collado, R., Monedero, E., 2020. Recirculation of char from biomass gasification: effects on gasifier performance and end-char properties. Renew. Energy 147, 806–813. https://doi.org/10.1016/j.renene.2019.09.063.
Hossain, M.A., Jewaratnam, J., Ganesan, P., 2016. Prospect of hydrogen production from oil palm biomass by thermochemical process – a review. Int. J. Hydrogen Energy 41, 16637–16655. https://doi.org/10.1016/j.ijhydene.2016.07.104.
Hu, M., Laghari, M., Cui, B., Xiao, B., Zhang, B., Guo, D., 2018. Catalytic cracking of biomass tar over char supported nickel catalyst. Energy 145, 228–237. https://doi.org/10.1016/j.energy.2017.12.096.
Hu, S., Jiang, L., Wang, Y., Su, S., Sun, L., Xu, B., He, L., Xiang, J., 2015. Effects of inherent alkali and alkaline earth metallic species on biomass pyrolysis at different temperatures. Bioresour. Technol. 192, 23–30. https://doi.org/10.1016/j.biortech.2015.05.042.
Huang, S., Liang, Q., Geng, J., Luo, H., Wei, Q., 2019. Sulfurized biochar prepared by simplified technic with superior adsorption property towards aqueous Hg(II) and adsorption mechanisms. Mater. Chem. Phys. 238, 121919. https://doi.org/10.1016/j.matchemphys.2019.121919.
Igalavithana, A.D., Mandal, S., Niazi, N.K., Vithanage, M., Parikh, S.J., Mukome, F.N., Rizwan, M., Oleszczuk, P., Al-Wabel, M., Bolan, N., Tsang, D.C., 2017. Advances and future directions of biochar characterization methods and applications. Crit. Rev. Environ. Sci. Technol. 47 (23), 2275–2330.
Imai, A., Hardi, F., Lundqvist, P., Furusjö, E., Kirtania, K., Karagöz, S., Tekin, K., Yoshikawa, K., 2018. Alkali-catalyzed hydrothermal treatment of sawdust for production of a potential feedstock for catalytic gasification. Appl. Energy 231, 594–599. https://doi.org/10.1016/j.apenergy.2018.09.150.
Jiang, Z., Zhang, X., Yuan, Z., Chen, J., Huang, B., Dionysiou, D.D., Yang, G., 2018. Enhanced photocatalytic CO2 reduction via the synergistic effect between Ag and activated carbon in TiO2/AC-Ag ternary composite. Chem. Eng. J. 348, 592–598. https://doi.org/10.1016/j.cej.2018.04.180.
Kang, K., Nanda, S., Hu, Y., 2022. Current trends in biochar application for catalytic conversion of biomass to biofuels. Catal. Today 404, 3–18. https://doi.org/10.1016/j.cattod.2022.06.033.
Karimi, S., Bibak, F., Meshkani, F., Rastegarpanah, A., Deng, J., Liu, Y., Dai, H., 2021. Promotional roles of second metals in catalyzing methane decomposition over the Ni-based catalysts for hydrogen production: a critical review. Int. J. Hydrogen Energy 46, 20435–20480. https://doi.org/10.1016/j.ijhydene.2021.03.160.
Kate, R., Khore, S., Chauhan, R., Kawade, U., Naik, S., Kale, B., Apte, S., 2021. Solid state low temperature synthesis approach for ZnO-ZnS nanoheterostructure with functionality as a photocatalyst for H2 production and for DSSC. J. Alloys Compd. 858, 158348. https://doi.org/10.1016/j.jallcom.2020.158348.
Khoo, C.G., Lam, M.K., Mohamed, A.R., Lee, K.T., 2020. Hydrochar production from high-ash low-lipid microalgal biomass via hydrothermal carbonization: effects of operational parameters and products characterization. Environ. Res. 188, 109828. https://doi.org/10.1016/j.envres.2020.109828.
Kołtowski, M., Charmas, B., Skubiszewska-Zięba, J., Oleszczuk, P., 2017. Effect of biochar activation by different methods on toxicity of soil contaminated by industrial activity. Ecotoxicol. Environ. Saf. 136, 119–125. https://doi.org/10.1016/j.ecoenv.2016.10.033.
Kumar, A., Singh, E., Mishra, R., Kumar, S., 2022. Biochar as environmental armour and its diverse role towards protecting soil, water and air. Sci. Total Environ. 806, 150444. https://doi.org/10.1016/j.scitotenv.2021.150444.
Kumar, A.N., Dissanayake, P.D., Masek, O., Priya, A., Ki Lin, C.S., Ok, Y.S., Kim, S.-H., 2021. Recent trends in biochar integration with anaerobic fermentation: win-win strategies in a closed-loop. Renew. Sustain. Energy Rev. 149, 111371. https://doi.org/10.1016/j.rser.2021.111371.
Kumar, M., Xiong, X., Sun, Y., Yu, I.K.M., Tsang, D.C.W., Hou, D., Gupta, J., Bhaskar, T., Pandey, A., 2020. Critical review on biochar-supported catalysts for pollutant degradation and sustainable biorefinery. Adv Sustain Syst 4, 1900149. https://doi.org/10.1002/adsu.201900149.
Kumi, A.G., Ibrahim, M.G., Nasr, M., Fujii, M., 2020. Biochar synthesis for industrial wastewater treatment: a critical review. Mater. Sci. Forum 1008, 202–212. https://doi.org/10.4028/www.scientific.net/MSF.1008.202.
Lam, S.S., Yek, P.N.Y., Ok, Y.S., Chong, C.C., Liew, R.K., Tsang, D.C.W., Park, Y.-K., Liu, Z., Wong, C.S., Peng, W., 2020. Engineering pyrolysis biochar via single-step microwave steam activation for hazardous landfill leachate treatment. J. Hazard Mater. 390, 121649. https://doi.org/10.1016/j.jhazmat.2019.121649.
Lee, D.-H., Hung, C.-P., 2012. Toward a clean energy economy: with discussion on role of hydrogen sectors. Int. J. Hydrogen Energy 37, 15753–15765. https://doi.org/10.1016/j.ijhydene.2012.02.064.
Lee, H.W., Kim, Y.M., Kim, S., Ryu, C., Park, S.H., Park, Y.K., 2018. Review of the use of activated biochar for energy and environmental applications. Carbon Letters. https://doi.org/10.5714/CL.2018.26.001.
Lee, J., Kim, K.-H., Kwon, E.E., 2017. Biochar as a catalyst. Renew. Sustain. Energy Rev. 77, 70–79. https://doi.org/10.1016/j.rser.2017.04.002.
Lee, J., Lee, K., Sohn, D., Kim, Y.M., Park, K.Y., 2018. Hydrothermal carbonization of lipid extracted algae for hydrochar production and feasibility of using hydrochar as a solid fuel. Energy 153, 913–920. https://doi.org/10.1016/j.energy.2018.04.112.
Li, J., Qiao, Y., Chen, X., Zong, P., Qin, S., Wu, Y., Wang, S., Zhang, H., Tian, Y., 2019. Steam gasification of land, coastal zone and marine biomass by thermal gravimetric analyzer and a free-fall tubular gasifier: biochars reactivity and hydrogen-rich syngas production. Bioresour. Technol. 289, 121495. https://doi.org/10.1016/j.biortech.2019.121495.
Li, L., Jiang, X., Wang, H., Wang, J., Song, Z., Zhao, X., Ma, C., 2017. Methane dry and mixed reforming on the mixture of bio-char and nickel-based catalyst with microwave assistance. J. Anal. Appl. Pyrolysis 125, 318–327. https://doi.org/10.1016/j.jaap.2017.03.009.
Li, L., Wang, H., Jiang, X., Song, Z., Zhao, X., Ma, C., 2016. Microwave-enhanced methane combined reforming by CO 2 and H 2 O into syngas production on biomass-derived char. Fuel 185, 692–700. https://doi.org/10.1016/j.fuel.2016.07.098.
Li, L., Yan, K., Chen, J., Feng, T., Wang, F., Wang, J., Song, Z., Ma, C., 2019. Fe-rich biomass derived char for microwave-assisted methane reforming with carbon dioxide. Sci. Total Environ. 657, 1357–1367. https://doi.org/10.1016/j.scitotenv.2018.12.097.
Li, L., Yang, Z., Chen, J., Qin, X., Jiang, X., Wang, F., Song, Z., Ma, C., 2018. Performance of bio-char and energy analysis on CH4 combined reforming by CO2 and H2O into syngas production with assistance of microwave. Fuel 215, 655–664. https://doi.org/10.1016/j.fuel.2017.11.107.
Li, M., Liu, C., Cao, H., Zhao, H., Zhang, Y., Fan, Z., 2014. KOH self-templating synthesis of three-dimensional hierarchical porous carbon materials for high performance supercapacitors. J Mater Chem A Mater 2, 14844. https://doi.org/10.1039/C4TA02167C.
Li, W., Cheng, C., He, L., Liu, M., Cao, G., Yang, S., Ren, N., 2021. Effects of feedstock and pyrolysis temperature of biochar on promoting hydrogen production of ethanol-type fermentation. Sci. Total Environ. 790, 148206. https://doi.org/10.1016/j.scitotenv.2021.148206.
Li, W., He, L., Cheng, C., Cao, G., Ren, N., 2020. Effects of biochar on ethanol-type and butyrate-type fermentative hydrogen productions. Bioresour. Technol. 306, 123088. https://doi.org/10.1016/j.biortech.2020.123088.
Li, X., Wang, C., Zhang, J., Liu, J., Liu, B., Chen, G., 2020. Preparation and application of magnetic biochar in water treatment: a critical review. Sci. Total Environ. 711, 134847. https://doi.org/10.1016/j.scitotenv.2019.134847.
Lian, W., Li, H., Yang, J., Joseph, S., Bian, R., Liu, X., Zheng, J., Drosos, M., Zhang, X., Li, L., Shan, S., Pan, G., 2021. Influence of pyrolysis temperature on the cadmium and lead removal behavior of biochar derived from oyster shell waste. Bioresour. Technol. Rep. 15, 100709. https://doi.org/10.1016/j.biteb.2021.100709.
Liu, J., Jiang, J., Meng, Y., Aihemaiti, A., Xu, Y., Xiang, H., Gao, Y., Chen, X., 2020. Preparation, environmental application and prospect of biochar-supported metal nanoparticles: a review. J. Hazard Mater. 388, 122026. https://doi.org/10.1016/j.jhazmat.2020.122026.
Liu, W.-J., Jiang, H., Yu, H.-Q., 2019. Emerging applications of biochar-based materials for energy storage and conversion. Energy Environ. Sci. 12, 1751–1779. https://doi.org/10.1039/C9EE00206E.
Liu, W.-J., Jiang, H., Yu, H.-Q., 2015. Development of biochar-based functional materials: toward a sustainable platform carbon material. Chem Rev 115, 12251–12285. https://doi.org/10.1021/acs.chemrev.5b00195.
Liu, W.-J., Ling, L., Wang, Y.-Y., He, H., He, Y.-R., Yu, H.-Q., Jiang, H., 2016. One-pot high yield synthesis of Ag nanoparticle-embedded biochar hybrid materials from waste biomass for catalytic Cr(<scp>vi</scp>) reduction. Environ. Sci.: Nano 3, 745–753. https://doi.org/10.1039/C6EN00109B.
Liu, W.-J., Zeng, F.-X., Jiang, H., Zhang, X.-S., 2011. Preparation of high adsorption capacity bio-chars from waste biomass. Bioresour. Technol. 102, 8247–8252. https://doi.org/10.1016/j.biortech.2011.06.014.

Lyu, H., Zhang, Q., Shen, B., 2020. Application of biochar and its composites in catalysis. Chemosphere 240, 124842. https://doi.org/10.1016/j.chemosphere.2019.124842.
Mao, Y., Gao, Y., Dong, W., Wu, H., Song, Z., Zhao, X., Sun, J., Wang, W., 2020. Hydrogen production via a two-step water splitting thermochemical cycle based on metal oxide – a review. Appl. Energy 267, 114860. https://doi.org/10.1016/j.apenergy.2020.114860.
Matos, J., 2016. Eco-friendly heterogeneous photocatalysis on biochar-based materials under solar irradiation. Top. Catal. 59, 394–402. https://doi.org/10.1007/s11244-015-0434-5.
Matsagar, B.M., Yang, R.-X., Dutta, S., Ok, Y.S., Wu, K.C.-W., 2021. Recent progress in the development of biomass-derived nitrogen-doped porous carbon. J Mater Chem A Mater 9, 3703–3728. https://doi.org/10.1039/D0TA09706C.
Mian, M.M., Liu, G., 2018. Recent progress in biochar-supported photocatalysts: synthesis, role of biochar, and applications. RSC Adv. 8, 14237–14248. https://doi.org/10.1039/C8RA02258E.
Michalak, I., Baśladyńska, S., Mokrzycki, J., Rutkowski, P., 2019. Biochar from A Freshwater macroalga as A potential biosorbent for wastewater treatment. Water (Basel) 11, 1390. https://doi.org/10.3390/w11071390.
Mishra, R., Kumar, A., Singh, E., Kumar, S., 2023a. Recent research advancements in catalytic pyrolysis of plastic waste. ACS Sustain Chem Eng 11, 2033–2049. https://doi.org/10.1021/acssuschemeng.2c05759.
Mishra, R., Kumar, S., 2023. Application of carbon-based adsorbents for landfill leachate treatment. In: Landfill Leachate Management. IWA Publishing, pp. 213–242. https://doi.org/10.2166/9781789063318_0213.
Mishra, R., Ong, H.C., Lin, C.-W., 2023b. Progress on co-processing of biomass and plastic waste for hydrogen production. Energy Convers. Manag. 284, 116983. https://doi.org/10.1016/j.enconman.2023.116983.
Mishra, R., Shu, C.M., Gollakota, A.R., Pan, S.Y., 2024. Unveiling the potential of pyrolysis-gasification for hydrogen-rich syngas production from biomass and plastic waste. Energy Convers. Manag. 321, 118997. https://doi.org/10.1016/j.enconman.2024.118997.
Mishra, R., Singh, E., Kumar, A., Ghosh, A., Lo, S.-L., Kumar, S., 2022. Co-gasification of solid waste and its impact on final product yields. J. Clean. Prod. 374, 133989. https://doi.org/10.1016/j.jclepro.2022.133989.
Mohan, D., Sarswat, A., Ok, Y.S., Pittman, C.U., 2014. Organic and inorganic contaminants removal from water with biochar, a renewable, low cost and sustainable adsorbent – a critical review. Bioresour. Technol. 160, 191–202. https://doi.org/10.1016/j.biortech.2014.01.120.
Mullen, C.A., Boateng, A.A., Goldberg, N.M., Lima, I.M., Laird, D.A., Hicks, K.B., 2010. Bio-oil and bio-char production from corn cobs and stover by fast pyrolysis. Biomass Bioenergy 34, 67–74. https://doi.org/10.1016/j.biombioe.2009.09.012.
Muradov, N., Fidalgo, B., Gujar, A.C., Garceau, N., T-Raissi, A., 2012. Production and characterization of Lemna minor bio-char and its catalytic application for biogas reforming. Biomass Bioenergy 42, 123–131. https://doi.org/10.1016/j.biombioe.2012.03.003.
Nakajima, K., Hara, M., 2012. Amorphous carbon with SO_3H groups as a solid brønsted acid catalyst. ACS Catal. 2, 1296–1304. https://doi.org/10.1021/cs300103k.
Nanda, S., Reddy, S.N., Mitra, S.K., Kozinski, J.A., 2016. The progressive routes for carbon capture and sequestration. Energy Sci. Eng. 4, 99–122. https://doi.org/10.1002/ese3.117.
Nguyen, H.K.D., Pham, V.V., Do, H.T., 2016. Preparation of Ni/biochar catalyst for hydrotreating of bio-oil from microalgae biomass. Catal Letters 146, 2381–2391. https://doi.org/10.1007/s10562-016-1873-8.
Nguyen, H.M., Sunarso, J., Li, C., Pham, G.H., Phan, C., Liu, S., 2020. Microwave-assisted catalytic methane reforming: a review. Appl. Catal. Gen. 599, 117620. https://doi.org/10.1016/j.apcata.2020.117620.
Nguyen, V.N., Sharma, P., Rowinski, L., Le, H.C., Le, D.T.N., Osman, S.M., Le, H.S., Truong, T.H., Nguyen, P.Q.P., Cao, D.N., 2024. Biochar-based catalysts derived from biomass waste: production, characterization, and application for liquid biofuel synthesis. Biofuels, Bioproducts and Biorefining. https://doi.org/10.1002/bbb.2593.
Norouzi, O., Kheradmand, A., Jiang, Y., Di Maria, F., Masek, O., 2019. Superior activity of metal oxide biochar composite in hydrogen evolution under artificial solar irradiation: a promising alternative to conventional metal-based photocatalysts. Int. J. Hydrogen Energy 44, 28698–28708. https://doi.org/10.1016/j.ijhydene.2019.09.119.
Oliveira, I., Blöhse, D., Ramke, H.-G., 2013. Hydrothermal carbonization of agricultural residues. Bioresour. Technol. 142, 138–146. https://doi.org/10.1016/j.biortech.2013.04.125.
Omidi, A.H., Cheraghi, M., Lorestani, B., Sobhanardakani, S., Jafari, A., 2019. Biochar obtained from cinnamon and cannabis as effective adsorbents for removal of lead ions from water. Environ. Sci. Pollut. Control Ser. 26, 27905–27914. https://doi.org/10.1007/s11356-019-05997-z.
Ormsby, R., Kastner, J.R., Miller, J., 2012. Hemicellulose hydrolysis using solid acid catalysts generated from biochar. Catal. Today 190, 89–97. https://doi.org/10.1016/j.cattod.2012.02.050.
Pak, T., Gomari, K.E., Bose, S., Tonon, T., Hughes, D., Gronnow, M., Macquarrie, D., 2023. Biochar from brown algae: production, activation, and characterisation. Bioresour. Technol. Rep. 24, 101688. https://doi.org/10.1016/j.biteb.2023.101688.
Pandey, B., Prajapati, Y.K., Sheth, P.N., 2019. Recent progress in thermochemical techniques to produce hydrogen gas from biomass: a state of the art review. Int. J. Hydrogen Energy 44, 25384–25415. https://doi.org/10.1016/j.ijhydene.2019.08.031.
Park, S., Jae, J., Farooq, A., Kwon, E.E., Park, E.D., Ha, J.-M., Jung, S.-C., Park, Y.-K., 2019. Continuous pyrolysis of organosolv lignin and application of biochar on gasification of high density polyethylene. Appl. Energy 255, 113801. https://doi.org/10.1016/j.apenergy.2019.113801.
Patel, S., Kundu, S., Halder, P., Marzbali, M.H., Chiang, K., Surapaneni, A., Shah, K., 2020. Production of hydrogen by catalytic methane decomposition using biochar and activated char produced from biosolids pyrolysis. Int. J. Hydrogen Energy 45, 29978–29992. https://doi.org/10.1016/j.ijhydene.2020.08.036.
Peterson, S.C., Jackson, M.A., 2014. Simplifying pyrolysis: using gasification to produce corn stover and wheat straw biochar for sorptive and horticultural media. Ind. Crops Prod. 53, 228–235. https://doi.org/10.1016/j.indcrop.2013.12.028.
Rahimpour, M.R., Jokar, S.M., 2012. Feasibility of flare gas reformation to practical energy in Farashband gas refinery: No gas flaring. J. Hazard Mater. 209–210, 204–217. https://doi.org/10.1016/j.jhazmat.2012.01.017.
Rathod, N., Jain, S., Patel, M.R., 2023. Thermodynamic analysis of biochar produced from groundnut shell through slow pyrolysis. Energy Nexus 9, 100177. https://doi.org/10.1016/j.nexus.2023.100177.
Ren, S., Lei, H., Wang, L., Bu, Q., Chen, S., Wu, J., 2014. Hydrocarbon and hydrogen-rich syngas production by biomass catalytic pyrolysis and bio-oil upgrading over biochar catalysts. RSC Adv. 4, 10731–10737. https://doi.org/10.1039/C4RA00122B.
Rezaeitavabe, F., Saadat, S., Talebbeydokhti, N., Sartaj, M., Tabatabaei, M., 2020. Enhancing bio-hydrogen production from food waste in single-stage hybrid dark-photo fermentation by addition of two waste materials (exhausted resin and biochar). Biomass Bioenergy 143, 105846. https://doi.org/10.1016/j.biombioe.2020.105846.
Romero, C.M., Li, C., Owens, J., Ribeiro, G.O., Mcallister, T.A., Okine, E., Hao, X., 2021. Nutrient cycling and greenhouse gas emissions from soil amended with biochar-manure mixtures. Pedosphere 31, 289–302. https://doi.org/10.1016/S1002-0160(20)60071-6.
Sabio, E., Álvarez-Murillo, A., Román, S., Ledesma, B., 2016. Conversion of tomato-peel waste into solid fuel by hydrothermal carbonization: influence of the processing variables. Waste Management 47, 122–132. https://doi.org/10.1016/j.wasman.2015.04.016.
Safari, F., Javani, N., Yumurtaci, Z., 2018. Hydrogen production via supercritical water gasification of almond shell over algal and agricultural hydrochars as catalysts. Int. J. Hydrogen Energy 43, 1071–1080. https://doi.org/10.1016/j.ijhydene.2017.05.102.
Saleem, Z., Pervaiz, E., Yousaf, M.U., Niazi, M.B.K., 2020. Two-Dimensional materials and composites as potential water splitting photocatalysts: a review. Catalysts 10, 464. https://doi.org/10.3390/catal10040464.
Sevilla, M., Fuertes, A.B., 2011. Sustainable porous carbons with a superior performance for CO2 capture. Energy Environ. Sci. 4, 1765. https://doi.org/10.1039/c0ee00784f.
Shan, R., Han, J., Gu, J., Yuan, H., Luo, B., Chen, Y., 2020. A review of recent developments in catalytic applications of biochar-based materials. Resour. Conserv. Recycl. 162, 105036. https://doi.org/10.1016/j.resconrec.2020.105036.
Sharma, P., Melkania, U., 2017. Biochar-enhanced hydrogen production from organic fraction of municipal solid waste using co-culture of Enterobacter aerogenes and E. coli. Int. J. Hydrogen Energy 42, 18865–18874. https://doi.org/10.1016/j.ijhydene.2017.06.171.
Shen, Q., Wu, H., 2023. Rapid pyrolysis of biochar prepared from slow and fast pyrolysis: the effects of particle residence time on char properties. Proc. Combust. Inst. 39, 3371–3378. https://doi.org/10.1016/j.proci.2022.07.119.
Shen, Y., 2015. Chars as carbonaceous adsorbents/catalysts for tar elimination during biomass pyrolysis or gasification. Renew. Sustain. Energy Rev. 43, 281–295. https://doi.org/10.1016/j.rser.2014.11.061.
Shen, Y., Chen, M., Sun, T., Jia, J., 2015. Catalytic reforming of pyrolysis tar over metallic nickel nanoparticles embedded in pyrochar. Fuel 159, 570–579. https://doi.org/10.1016/j.fuel.2015.07.007.
Shen, Y., Fu, Y., 2018. Advances in *in situ* and *ex situ* tar reforming with biochar catalysts for clean energy production. Sustain. Energy Fuels 2, 326–344. https://doi.org/10.1039/C7SE00553A.
Shi, C., Ye, S., Wang, X., Meng, F., Liu, Junxue, Yang, T., Zhang, W., Wei, J., Ta, N., Lu, G. Q. Max, Hu, M., Liu, Jian, 2021. Modular construction of prussian blue analog and TiO_2 dual-compartment janus nanoreactor for efficient photocatalytic water splitting. Adv. Sci. 8, 2001987. https://doi.org/10.1002/advs.202001987.
Shi, X., Li, P., Wang, X., Song, J., Fang, S., Chang, C., Pang, S., 2022. Enhancement of the production of aromatics and bio-syngas from microwave ex-situ pyrolysis based on Zn/Zr modified biochar and multi-catalysts. Energy 261, 125307. https://doi.org/10.1016/j.energy.2022.125307.
Silva, R.D.V.K., Lei, Z., Shimizu, K., Zhang, Z., 2020. Hydrothermal treatment of sewage sludge to produce solid biofuel: focus on fuel characteristics. Bioresour. Technol. Rep. 11, 100453. https://doi.org/10.1016/j.biteb.2020.100453.
Singh, E., Kumar, A., Mishra, R., You, S., Singh, L., Kumar, S., Kumar, R., 2021. Pyrolysis of waste biomass and plastics for production of biochar and its use for removal of heavy metals from aqueous solution. Bioresour. Technol. 320, 124278. https://doi.org/10.1016/j.biortech.2020.124278.
Sofi'i, Y.K., Siswanto, E., Winarto, W., Wardana, I.N.G., 2020. Development of bamboo charcoal and fragaria vesca powder photocatalysts in hydrogen production via water splitting. E. Eur. J. Enterprise Technol. 6, 80–92. https://doi.org/10.15587/1729-4061.2020.213277.
Song, B., Cao, X., Gao, W., Aziz, S., Gao, S., Lam, C.-H., Lin, R., 2022. Preparation of nano-biochar from conventional biorefineries for high-value applications. Renew. Sustain. Energy Rev. 157, 112057. https://doi.org/10.1016/j.rser.2021.112057.
Sugiarto, Y., Sunyoto, N.M.S., Zhu, M., Jones, I., Zhang, D., 2021. Effect of biochar in enhancing hydrogen production by mesophilic anaerobic digestion of food wastes: the role of minerals. Int. J. Hydrogen Energy 46, 3695–3703. https://doi.org/10.1016/j.ijhydene.2020.10.256.
Sun, K., Huang, Q., Ali, M., Chi, Y., Yan, J., 2018. Producing aromatic-enriched oil from mixed plastics using activated biochar as catalyst. Energy & Fuels 32, 5471–5479. https://doi.org/10.1021/acs.energyfuels.7b03710.

Sunyoto, N.M.S., Zhu, M., Zhang, Z., Zhang, D., 2017. Effect of biochar addition and initial pH on hydrogen production from the first phase of two-phase anaerobic digestion of carbohydrates food waste. Energy Proc. 105, 379–384. https://doi.org/10.1016/j.egypro.2017.03.329.

Taghavi, S., Norouzi, O., Tavasoli, A., Di Maria, F., Signoretto, M., Menegazzo, F., Di Michele, A., 2018. Catalytic conversion of Venice lagoon brown marine algae for producing hydrogen-rich gas and valuable biochemical using algal biochar and Ni/SBA-15 catalyst. Int. J. Hydrogen Energy 43, 19918–19929. https://doi.org/10.1016/j.ijhydene.2018.09.028.

Tang, S., Xia, Y., Fan, J., Cheng, B., Yu, J., Ho, W., 2021. Enhanced photocatalytic H2 production performance of CdS hollow spheres using C and Pt as bi-cocatalysts. Chin. J. Catal. 42, 743–752. https://doi.org/10.1016/S1872-2067(20)63695-6.

Tauqir, W., Zubair, M., Nazir, H., 2019. Parametric analysis of a steady state equilibrium-based biomass gasification model for syngas and biochar production and heat generation. Energy Convers. Manag. 199, 111954. https://doi.org/10.1016/j.enconman.2019.111954.

Te, W.Z., Muhanin, K.N.M., Chu, Y.-M., Selvarajoo, A., Singh, A., Ahmed, S.F., Vo, D.-V. N., Show, P.L., 2021. Optimization of pyrolysis parameters for production of biochar from banana peels: evaluation of biochar application on the growth of Ipomoea aquatica. Front. Energy Res. 8. https://doi.org/10.3389/fenrg.2020.637846.

Tian, H., Hu, Q., Wang, J., Chen, D., Yang, Y., Bridgwater, A.V., 2021. Kinetic study on the CO2 gasification of biochar derived from Miscanthus at different processing conditions. Energy 217, 119341. https://doi.org/10.1016/j.energy.2020.119341.

Tian, K., Liu, W.-J., Zhang, S., Jiang, H., 2016. One-pot synthesis of a carbon supported bimetallic Cu–Ag NPs catalyst for robust catalytic hydroxylation of benzene to phenol by fast pyrolysis of biomass waste. Green Chem. 18, 5643–5650. https://doi.org/10.1039/C6GC01231K.

Toloue Farrokh, N., Suopajärvi, H., Mattila, O., Umeki, K., Phounglamcheik, A., Romar, H., Sulasalmi, P., Fabritius, T., 2018. Slow pyrolysis of by-product lignin from wood-based ethanol production– A detailed analysis of the produced chars. Energy 164, 112–123. https://doi.org/10.1016/j.energy.2018.08.161.

Tu, X., Whitehead, J.C., 2012. Plasma-catalytic dry reforming of methane in an atmospheric dielectric barrier discharge: understanding the synergistic effect at low temperature. Appl. Catal., B 125, 439–448. https://doi.org/10.1016/j.apcatb.2012.06.006.

Waheed, Q.M.K., Williams, P.T., 2013. Hydrogen production from high temperature pyrolysis/steam reforming of waste biomass: rice husk, sugar cane bagasse, and wheat straw. Energy & Fuels 27, 6695–6704. https://doi.org/10.1021/ef401145w.

Wan, Z., Sun, Y., Tsang, D.C.W., Hou, D., Cao, X., Zhang, S., Gao, B., Ok, Y.S., 2020. Sustainable remediation with an electroactive biochar system: mechanisms and perspectives. Green Chem. 22, 2688–2711. https://doi.org/10.1039/D0GC00717J.

Wang, C., Lei, H., Kong, X., Zou, R., Qian, M., Zhao, Y., Mateo, W., 2021a. Catalytic upcycling of waste plastics over nanocellulose derived biochar catalyst for the coupling harvest of hydrogen and liquid fuels. Sci. Total Environ. 779, 146463. https://doi.org/10.1016/j.scitotenv.2021.146463.

Wang, C., Lei, H., Qian, M., Huo, E., Zhao, Y., Zhang, Q., Mateo, W., Lin, X., Kong, X., Zou, R., Ruan, R., 2020a. Application of highly stable biochar catalysts for efficient pyrolysis of plastics: a readily accessible potential solution to a global waste crisis. Sustain. Energy Fuels 4, 4614–4624. https://doi.org/10.1039/D0SE00652A.

Wang, C., Lei, H., Qian, M., Huo, E., Zhao, Y., Zhang, Q., Mateo, W., Lin, X., Kong, X., Zou, R., Ruan, R., 2020b. Application of highly stable biochar catalysts for efficient pyrolysis of plastics: a readily accessible potential solution to a global waste crisis. Sustain. Energy Fuels 4, 4614–4624. https://doi.org/10.1039/D0SE00652A.

Wang, C., Lei, H., Zhao, Y., Qian, M., Kong, X., Mateo, W., Zou, R., Ruan, R., 2021b. Integrated harvest of phenolic monomers and hydrogen through catalytic pyrolysis of biomass over nanocellulose derived biochar catalyst. Bioresour. Technol. 320, 124352. https://doi.org/10.1016/j.biortech.2020.124352.

Wang, D., Yuan, W., Ji, W., 2011. Char and char-supported nickel catalysts for secondary syngas cleanup and conditioning. Appl. Energy 88, 1656–1663. https://doi.org/10.1016/j.apenergy.2010.11.041.

Wang, G., Li, Q., Dzakpasu, M., Gao, X., Yuwen, C., Wang, X.C., 2018. Impacts of different biochar types on hydrogen production promotion during fermentative co-digestion of food wastes and dewatered sewage sludge. Waste Management 80, 73–80. https://doi.org/10.1016/j.wasman.2018.08.042.

Wang, H., Lou, X., Hu, Q., Sun, T., 2021. Adsorption of antibiotics from water by using Chinese herbal medicine residues derived biochar: preparation and properties studies. J. Mol. Liq. 325, 114967. https://doi.org/10.1016/j.molliq.2020.114967.

Wang, H., Qu, M., Wang, S., Liu, X., Li, L., 2019. Fabrication of high-performance biomass derived carbon/metal oxide photocatalysts with trilevel hierarchical pores from organic–inorganic network. Adv Sustain Syst 3, 1800169. https://doi.org/10.1002/adsu.201800169.

Wang, J., Kaskel, S., 2012. KOH activation of carbon-based materials for energy storage. J. Mater. Chem. 22, 23710. https://doi.org/10.1039/c2jm34066f.

Wang, J., Yin, Y., 2017. Biohydrogen Production from Organic Wastes. Springer Singapore, Singapore. https://doi.org/10.1007/978-981-10-4675-9.

Wang, Q., Cai, J., Biesold-McGee, G.V., Huang, J., Ng, Y.H., Sun, H., Wang, J., Lai, Y., Lin, Z., 2020. Silk fibroin-derived nitrogen-doped carbon quantum dots anchored on TiO2 nanotube arrays for heterogeneous photocatalytic degradation and water splitting. Nano Energy 78, 105313. https://doi.org/10.1016/j.nanoen.2020.105313.

Wang, S., Wang, Y., Zhang, S.L., Zang, S., Lou, X.W.David, 2019. Supporting ultrathin $ZnIn_2S_4$ nanosheets on Co/N-doped graphitic carbon nanocages for efficient photocatalytic H_2 generation. Adv. Mater. 31, 1903404. https://doi.org/10.1002/adma.201903404.

Wang, Y., Huang, L., Zhang, T., Wang, Q., 2022. Hydrogen-rich syngas production from biomass pyrolysis and catalytic reforming using biochar-based catalysts. Fuel 313, 123006. https://doi.org/10.1016/j.fuel.2021.123006.

Weerachanchai, P., Horio, M., Tangsathitkulchai, C., 2009. Effects of gasifying conditions and bed materials on fluidized bed steam gasification of wood biomass. Bioresour. Technol. 100, 1419–1427. https://doi.org/10.1016/j.biortech.2008.08.002.

Wen, C., Liu, T., Wang, D., Wang, Y., Chen, H., Luo, G., Zhou, Z., Li, C., Xu, M., 2023. Biochar as the effective adsorbent to combustion gaseous pollutants: preparation, activation, functionalization and the adsorption mechanisms. Prog. Energy Combust. Sci. 99, 101098. https://doi.org/10.1016/j.pecs.2023.101098.

Xiang, Z., Nan, J., Deng, J., Shi, Y., Zhao, Y., Zhang, B., Xiang, X., 2019. Uniform CdS-decorated carbon microsheets with enhanced photocatalytic hydrogen evolution under visible-light irradiation. J. Alloys Compd. 770, 886–895. https://doi.org/10.1016/j.jallcom.2018.08.214.

Xiao, X., Cao, J., Meng, X., Le, D.D., Li, L., Ogawa, Y., Sato, K., Takarada, T., 2013. Synthesis gas production from catalytic gasification of waste biomass using nickel-loaded brown coal char. Fuel 103, 135–140. https://doi.org/10.1016/j.fuel.2011.06.077.

Xie, J., Xia, H., Guan, M., Huang, K., Chen, J., 2023. Accelerating the humification mechanism of dissolved organic matter using biochar during vermicomposting of dewatered sludge. Waste Management 159, 102–113. https://doi.org/10.1016/j.wasman.2023.01.022.

Xu, M., Kang, Y., Jiang, Linlin, Jiang, Lei, Tremblay, P.-L., Zhang, T., 2022. The one-step hydrothermal synthesis of CdS nanorods modified with carbonized leaves from Japanese raisin trees for photocatalytic hydrogen evolution. Int. J. Hydrogen Energy 47, 15516–15527. https://doi.org/10.1016/j.ijhydene.2021.09.023.

Xu, R., Yan, C., Liu, Q., Liu, E., Zhang, H., Zhang, Xiaoxiao, Yuan, X., Han, L., Lei, H., Ruan, R., Zhang, Xuesong, 2022. Development of metal-doping mesoporous biochar catalyst for co-valorizing biomass and plastic waste into valuable hydrocarbons, syngas, and carbons. Fuel Process. Technol. 227, 107127. https://doi.org/10.1016/j.fuproc.2021.107127.

Yaashikaa, P.R., Kumar, P.S., Varjani, S., Saravanan, A., 2020. A critical review on the biochar production techniques, characterization, stability and applications for circular bioeconomy. Biotechnology Reports 28, e00570. https://doi.org/10.1016/j.btre.2020.e00570.

Yaashikaa, P.R., Senthil Kumar, P., Varjani, S.J., Saravanan, A., 2019. Advances in production and application of biochar from lignocellulosic feedstocks for remediation of environmental pollutants. Bioresour. Technol. 292, 122030. https://doi.org/10.1016/j.biortech.2019.122030.

Yan, W., Hastings, J.T., Acharjee, T.C., Coronella, C.J., Vásquez, V.R., 2010. Mass and energy balances of wet torrefaction of lignocellulosic biomass. Energy & Fuels 24, 4738–4742. https://doi.org/10.1021/ef901273n.

Yang, G., Wang, J., 2019. Synergistic enhancement of biohydrogen production from grass fermentation using biochar combined with zero-valent iron nanoparticles. Fuel 251, 420–427. https://doi.org/10.1016/j.fuel.2019.04.059.

Yao, D., Hu, Q., Wang, D., Yang, H., Wu, C., Wang, X., Chen, H., 2016. Hydrogen production from biomass gasification using biochar as a catalyst/support. Bioresour. Technol. 216, 159–164. https://doi.org/10.1016/j.biortech.2016.05.011.

Yao, Q., Borjihan, Q., Qu, H., Guo, Y., Zhao, Z., Qiao, L., Li, T., Dong, A., Liu, Y., 2021. Cow dung-derived biochars engineered as antibacterial agents for bacterial decontamination. Journal of Environmental Sciences 105, 33–43. https://doi.org/10.1016/j.jes.2020.12.022.

Yao, Z., You, S., Ge, T., Wang, C.-H., 2018. Biomass gasification for syngas and biochar co-production: energy application and economic evaluation. Appl. Energy 209, 43–55. https://doi.org/10.1016/j.apenergy.2017.10.077.

Yoo, J.-H., Luyima, D., Lee, J.-H., Park, S.-Y., Yang, J.-W., An, J.-Y., Yun, Y.-U., Oh, T.-K., 2021. Effects of brewer's spent grain biochar on the growth and quality of leaf lettuce (Lactuca sativa L. var. crispa.). Appl Biol Chem 64, 10. https://doi.org/10.1186/s13765-020-00577-z.

Yu, J.T., Dehkhoda, A.M., Ellis, N., 2011. Development of biochar-based catalyst for transesterification of canola oil. Energy & Fuels 25, 337–344. https://doi.org/10.1021/ef100977d.

Yu, X., Zhou, H., Ye, X., Wang, H., 2021. From hazardous agriculture waste to hazardous metal scavenger: tobacco stalk biochar-mediated sequestration of Cd leads to enhanced tobacco productivity. J. Hazard Mater. 413, 125303. https://doi.org/10.1016/j.jhazmat.2021.125303.

Zeng, Y., Zhu, X., Mei, D., Ashford, B., Tu, X., 2015. Plasma-catalytic dry reforming of methane over γ-Al2O3 supported metal catalysts. Catal. Today 256, 80–87. https://doi.org/10.1016/j.cattod.2015.02.007.

Zha, D.-W., Li, L.-F., Pan, Y.-X., He, J.-B., 2016. Coconut shell carbon nanosheets facilitating electron transfer for highly efficient visible-light-driven photocatalytic hydrogen production from water. Int. J. Hydrogen Energy 41, 17370–17379. https://doi.org/10.1016/j.ijhydene.2016.07.227.

Zhang, J., Fan, C., Zang, L., 2017. Improvement of hydrogen production from glucose by ferrous iron and biochar. Bioresour. Technol. 245, 98–105. https://doi.org/10.1016/j.biortech.2017.08.198.

Zhang, J., Zhao, X., Wang, Y., Gong, Y., Cao, D., Qiao, M., 2018. Peroxymonosulfate-enhanced visible light photocatalytic degradation of bisphenol A by perylene imide-modified g-C3N4. Appl. Catal., B 237, 976–985. https://doi.org/10.1016/j.apcatb.2018.06.049.

Zhao, L., Chen, C., Ren, H.-Y., Wu, J.-T., Meng, J., Nan, J., Cao, G.-L., Yang, S.-S., Ren, N.-Q., 2020. Feasibility of enhancing hydrogen production from cornstalk hydrolysate anaerobic fermentation by RCPH-biochar. Bioresour. Technol. 297, 122505. https://doi.org/10.1016/j.biortech.2019.122505.

Zhao, L., Wang, Z., Ren, H.-Y., Chen, C., Nan, J., Cao, G.-L., Yang, S.-S., Ren, N.-Q., 2021a. Residue cornstalk derived biochar promotes direct bio-hydrogen production from anaerobic fermentation of cornstalk. Bioresour. Technol. 320, 124338. https://doi.org/10.1016/j.biortech.2020.124338.

Zhao, L., Wu, K.-K., Chen, C., Ren, H.-Y., Wang, Z.-H., Nan, J., Yang, S.-S., Cao, G.-L., Ren, N.-Q., 2021b. Role of residue cornstalk derived biochar for the enhanced bio-hydrogen production via simultaneous saccharification and fermentation of cornstalk. Bioresour. Technol. 330, 125006. https://doi.org/10.1016/j.biortech.2021.125006.

Zhao, S., Zhang, L., Hu, H., Jin, L., 2023. Catalytic decomposition of methane over enteromorpha prolifera-based hierarchical porous biochar. Int. J. Hydrogen Energy 48, 3328–3339. https://doi.org/10.1016/j.ijhydene.2022.10.215.

Zheng, Q., Wang, P., Zhu, Y., Ji, B., Mao, T., Fang, Y., Zhang, X., Wang, Z., Yang, H., 2021. A novel sensitized matrix Pythium oligandrum-derived carbon for enhancement photocatalytic hydrogen evolution. Mater. Lett. 284, 128939. https://doi.org/10.1016/j.matlet.2020.128939.